CONTAINERLESS PROCESSING OF BERYLLIUM

EXPERIMENT 74-48

Contract No. NAS8-31963

FINAL REPORT

June 1977

Prepared for

National Aeronautics and Space Administration
George C. Marshall Space Flight Center

Space Sciences Laboratory
General Electric Space Division
P.O. Box 8555, Philadelphia, Pa. 19101

and

Kawecki Berylco Industries, Inc.
P.O. Box 1462, Reading, Pa. 19603
Subcontractor

CONTAINERLESS PROCESSING OF BERYLLIUM

EXPERIMENT 74-48

by

Gerald Wouch
George H. Keith
Robert T. Frost
Norman P. Pinto

Space Sciences Laboratory
General Electric Space Division
P. O. Box 8555, Philadelphia, Pa. 19101

and

Kawecki Berylco Industries, Inc.
P. O. Box 1462, Reading, Pa. 19603
Subcontractor

TABLE OF CONTENTS

ABSTRACT

Melting and solidification of a beryllium alloy containing 1.5% BeO by weight in the weightless environment of space has produced a new material not produced terrestrially, to our knowledge, namely cast beryllium with a relatively uniform dispersion of BeO throughout. Examination of the cast material shows that it is coarse grained, although the BeO is not heavily agglomerated in the flight specimen. Ground based comparison experiments show extreme agglomeration and segregation of BeO, resulting in large zones which are practically free of the oxide. Several postulated hypotheses for the failure to grain refine the beryllium have been formulated. These are: (1) spherodization of the BeO particles during specimen preparation and during the molten phase of the experiment; (2) loss of nucleation potency through aging in the molten phase; and (3) inability of BeO to act as a grain refiner for beryllium. Further investigation with non-spherodized particles and shorter dwell times molten may delineate which of these hypotheses are valid. The results of this flight experiment indicate that the weightless environment of space is an important asset in conducting research to find grain refiners for beryllium and other metals for which cast dispersions of grain refining agents cannot be prepared terrestrially due to gravitationally driven settling and agglomeration.

SUMMARY

This report describes preparatory ground based research and a subsequent sounding rocket experiment wherein beryllium alloy HP-50 was melted and solidified in the weightless environment of space in the NASA Electromagnetic Containerless Processing Payload on SPAR III. During that experiment, successful melting and solidification was achieved. Although a stiff oxide layer formed on the specimen due to the lack of a clean vacuum environment for the specimen in this first containerless experiment, the technique allowed rapid radiative cooling and solidification of the specimen and pyrometric observation of the specimen surface without interference from a container or hot oven walls.

Comparisons with ground based produced specimens show that the flight specimen has a much more uniform distribution of BeO and is essentially unagglomerated. Heavy agglomeration and separation was produced in the ground based reference experiments. The results of metallographic investigations and scanning electron microscopy are presented below.

It was observed that while the BeO distribution was uniform and unagglomerated in the flight specimen, grain refinement did not occur and the castings are coarse grained. Several hypotheses requiring further investigation have been formulated to explain the failure to produce a relatively fine grained casting. These experiments would require a shorter dwell time while molten and utilize material prepared so that BeO particles with smooth facets with sharp corners were present initially.

Whereas many potential grain refining agents for beryllium agglomerate and segregate from the melt terrestrially due to (1) Stokes collisions and (2) velocity gradient collisions, this experiment indicates that the weightless environment of space is an important asset for conducting research to assess the potency of these agents as grain refiners. The results show that

agglomeration and separation times are greatly extended in the weightless environment of space due to the reduction in collision frequency through gravity driven mechanisms such as Stokes Collisions and fluid motions induced by gravity driven convection.

SECTION 1
INTRODUCTION

Cast beryllium is coarse grained and, consequently, brittle. Subsequent hot working is required to refine the grain structure before cast beryllium can be used for most applications. Because of the problems in casting and subsequent hot working the cast beryllium, powder metallurgy is resorted to. Beryllium metal is principally produced in final form by consolidating a fine powder, usually #200 or 300 mesh; i.e., 77 or 44 μm, respectively, either by vacuum hot-pressing or by hot-isopressing. Occasionally, standard cold pressing and sintering techniques are used to produce some material. Some cast metal is used after hot working, particularly where its purity and cleanliness cannot be matched by the powder metallurgical product.

The desirability of obtaining fine grained castings of beryllium with good mechanical behavior has spurred research to find a suitable grain refining agent for beryllium. Based on classical heterogeneous nucleation theory (Ref. 1), a good grain refining agent should: (1) have a relatively high surface energy between the particle and the melt; (2) have a low surface energy between the solid and the particle; (3) be stable in the molten metal; (4) possess a maximum of surface area; (5) have optimum surface character. Because of the lack of information (Ref. 1) about the majority of these parameters, attention has been mainly concentrated on lattice disregistry between the nucleating particle material and the solid. The surface energy between the solid and the particle should decrease with decreasing lattice mismatch between particle and solid and with increasing chemical affinity between particle and solid (Ref. 1). Empirically, then, the search for grain refiners for casting has begun with lattice disregistry between the particle and the solid.

Consequently, for beryllium, one logical choice of a grain refining agent is beryllia, BeO. Additionally it has been shown (Ref. 2) that the grain growth stabilization temperature of beryllium can be raised by an oxide dispersion, the extent being inversely proportional to the particle size of the oxide dispersion.

Thus beryllia might act both as a grain refining agent to produce fine grained beryllium and to stabilize the grains produced, preventing excessive grain growth at high temperatures after solidification.

Attempts to produce castings of beryllium with a uniform dispersion of beryllia, (BeO), terrestrially, have not been successful due to agglomeration in the liquid state of the oxide particles and subsequent segregation of BeO from the melt. Agglomeration may occur due to: (1) Stokes Collisions, which arise whenever larger particles rising or settling through the melt collect smaller particles and (2) Gradient Collisions, arising when particles are swept together by fluid flow. Stokes Collisions require the presence of a gravity field, while Gradient Collisions may originate from gravity induced fluid flows such as convection but may also originate from other sources of fluid flow. A discussion of these mechanisms has been presented by Lindborg and Torssell (Ref. 3). NASA Contract No. NAS8-29748 has also considered these collision mechanisms in respect to agglomeration in immiscible liquid systems.

In the weightless environment of space, the reduced gravity should considerably reduce the agglomeration due to Stokes Collisions and through reduction in gravity driven convection may also reduce agglomeration due to Gradient Collisions, although other sources of fluid motion such as Marangoni convection and stirring must be considered. Thus in the weightless environment of space, a uniform dispersion of beryllia might be obtained in cast beryllium. In light of these considerations, a sounding rocket experiment was flown on the NASA SPAR III sounding rocket. The experiment and the results of the experiment are discussed below.

1.1 EXPERIMENT OBJECTIVES

The experiment objectives were: (1) To prepare cast beryllium with enhanced service properties through utilization of dispersed oxide, BeO, as a grain refining agent. Obtaining a finer grained casting of beryllium with a uniform dispersion of oxide throughout would produce a cast beryllium with enhanced room

temperature ductility, coupled with high temperature strength. This would eliminate the present problems in subsequent hot working of the coarse grained castings presently produced to refine the cast structure. This goal has not been achievable in the terrestrial environment because of the unavoidable agglomeration and separation of beryllia, as well as other potential grain refining agents from the melt. (2) To improve the microstructure of cast beryllium. Achievement of a uniformly dispersed oxide phase in ingot beryllium may lead to enhancement of some service properties of beryllium even if grain refinement is not achieved, provided that grain sizes do not exceed perhaps 100 μm and do not grow when the material is worked. Obtaining a uniformly dispersed oxide phase of submicron sized particles may produce dispersion strengthened cast beryllium and (Ref. 2) stabilize against further grain growth at high temperatures. Achievement of a uniform dispersion of oxide can also demonstrate the feasibility of casting beryllium with additions other than BeO, e.g., titanium, tungsten, etc., as possible grain refining agents, in the weightless environment of space.

1.1.1 MINIMUM CRITERIA FOR SUCCESS

To measure the success of the experiment in terms of the experiment objectives discussed above, a set of minimum criteria for success was established. These were: (1) Satisfactory melting and solidification (minimum contamination from atmosphere, no contamination by contact, proper shape of casting). (2a) Improved cast microstructure - presence of a dispersed oxide phase in ingot beryllium. This will also indicate feasibility of using additions other than BeO, e.g., Ti, W (impossible in conventional melting). (2b) Improved cast microstructure - finer cast grain size. (3) Improved service properties.

1.2 GENERAL EXPERIMENT DESCRIPTION

The experimental program followed, leading up to the flight experiment, accomplished the necessary preliminaries to the flight experiment, including: (1) The selection of the flight specimen composition. (2) The establishment of cleanliness requirements during the melting and solidification, particularly with respect to water vapor and oxygen. (3) Ground based reference experiments,

representing the best attempt to simulate, terrestrially, the conditions of melting, cooling, and solidification occurring during the flight. The specimens obtained from the ground based reference experiments are the basis of comparison between the results of the flight experiment in the weightless environment of space and what can be achieved terrestrially. The results obtained in these ground based reference experiments were compared with previous experiments conducted in beryllium casting at KBI and also with the results of experiments conducted on NASA Contract No. NAS8-29626 (Ref. 4).

After establishing the necessary preliminary data, the flight specimen composition was selected (HIP-50 KBI alloy) to be a hot isostatically pressed beryllium alloy containing 1.5% BeO by weight. The flight experiment consisted of melting and solidification of a specimen of this composition in the NASA Electromagnetic Containerless Processing Payload (ECPP) developed for the SPAR program. The results of this experiment were then compared with that obtained from the ground based reference experiments performed.

1.2.1 GROUND BASED EXPERIMENT DESCRIPTION AND APPARATUS

Experiments in the terrestrial environment were performed in either a hot wall furnace at KBI or in the General Electric Breadboard Apparatus at KBI. The hot wall furnace was used to prepare a range of compositions of specimens by melting and solidifying a range of compositions of hot isostatically pressed beryllium alloys. The BeO content was varied from 0.6% BeO to 4.5% BeO by weight. Melting and cooling curves were obtained by optical pyrometry. As the thermal time constant is large in this furnace, the rapid heating and cooling capability of the Electromagnetic Containerless Processing Payload (ECPP) cannot be duplicated with this furnace. Thus in no way were these initial furnace experiments intended to serve as the ground based reference experiment. They did enable the grain size, agglomeration of beryllia, and homogeneity of product as functions of the initial composition and slower temperature-time kinetics to be studied. The metallographic studies of these specimens, reported below, enabled

the flight specimen composition to be chosen, 1.5% BeO by weight (KBI HIP-50 alloy) on the basis of smallest particle size obtained. All of these meltings were conducted with laboratory grade argon as the gaseous environment.

The General Electric Breadboard Apparatus was used to conduct the ground based reference experiments for melting and solidification of the HIP-50 beryllium alloy. The Breadboard Chamber contains a duplicate of the cusp coil and r.f. tank circuit used in the flight chamber. This apparatus is (as it is named) a breadboard of the ECPP, with a somewhat larger levitation chamber. The chamber can be evacuated to 10^{-6} torr and filled with high purity argon through a small vacuum/gas supply system designed for this purpose. A mass spectrometer such as the VEECO GA-4 Residual Gas Analyzer, may be coupled into the chamber to study the residual gases present in the chamber prior to and after filling with high purity argon.

Two ground based reference experiments, duplicating insofar as is possible terrestrially the flight experiments, were performed in this apparatus, heating, melting, and solidifying a specimen of the KBI HIP-50 beryllium alloy in the presence of high purity, research grade argon. These experiments were performed at KBI's laboratory in Reading, Pa. in a safe facility for beryllium, utilizing the Breadboard Apparatus. The specimens (0.922 cm in diameter spheroids of HIP-50 alloy) were sting mounted on a tungsten sting in the cusp coil. The specimens are heated and melted as in the flight apparatus by the r.f. induction field of the coil. Because beryllium is a light metal (density 1.848 gms/cm^3) enough levitation force is provided by the coil to support the specimens and they do not flow down the sting or fall when melted. Temperature is observed with the breadboard pyrometer, which is a duplicate of the flight pyrometer, and a disappearing filament pyrometer looking through the observation port down onto the specimen through the mirror system provided in the chamber for this purpose. The performance and results of these experiments are described below.

1.2.2 FLIGHT EXPERIMENT DESCRIPTION AND APPARATUS

The flight experiment consisted of melting and resolidification, under 18 psi of research grade argon, a 0.922 centimeter diameter, spheroidal specimen of KBI HIP-50 beryllium alloy, containing 1.5% BeO by weight, in the weightless environment of space. The experiment was performed in the NASA Electromagnetic Containerless Processing Payload (ECPP) flown on NASA SPAR III. A schematic of the ECPP is shown in Figure 1. Figures 2 and 3 show photographs of the ECPP and the levitation chamber respectively.

The specimen is suspended in the electromagnetic field of the cusp coil and heated and melted by induction heating from the electromagnetic field of the coil. The cusp coil consists of adjacent coils having opposing alternating magnetic fields. The potential well in which the specimen is confined is symmetrical about the vertical axis and roughly shaped as shown in Figure 4. An active servo positioning system is utilized to maintain the specimen in the center of the coil system against accelerations during the flight and to damp out oscillations of the specimen in the coil system. During the low power mode, after heating and melting, the specimen solidifies with very little stirring.

The rocket-borne apparatus is described in the End Item Specification, SSL-ECPP-001, prepared under NASA Contract NAS8-30797. Drawings of the apparatus are referenced in this document. Mechanical, electrical and functional interfaces with the rocket and pre-launch check-out equipment are detailed in the Final Interface Control Document, SSL-ECPP-009. Further information on the rocket-borne apparatus may be found in the final report for NASA Contract NAS8-30797 and the Experiment Implementation Plan for Containerless Processing of Beryllium, prepared for NASA Contract NAS8-31963.

The processing chamber was cleaned, evacuated and baked out for two days at 180°F. Mass spectrometric analysis of the residual gas showed less than 50 parts per million of water vapor and oxygen present after evacuation before filling with research grade argon. The research grade argon used contains less than

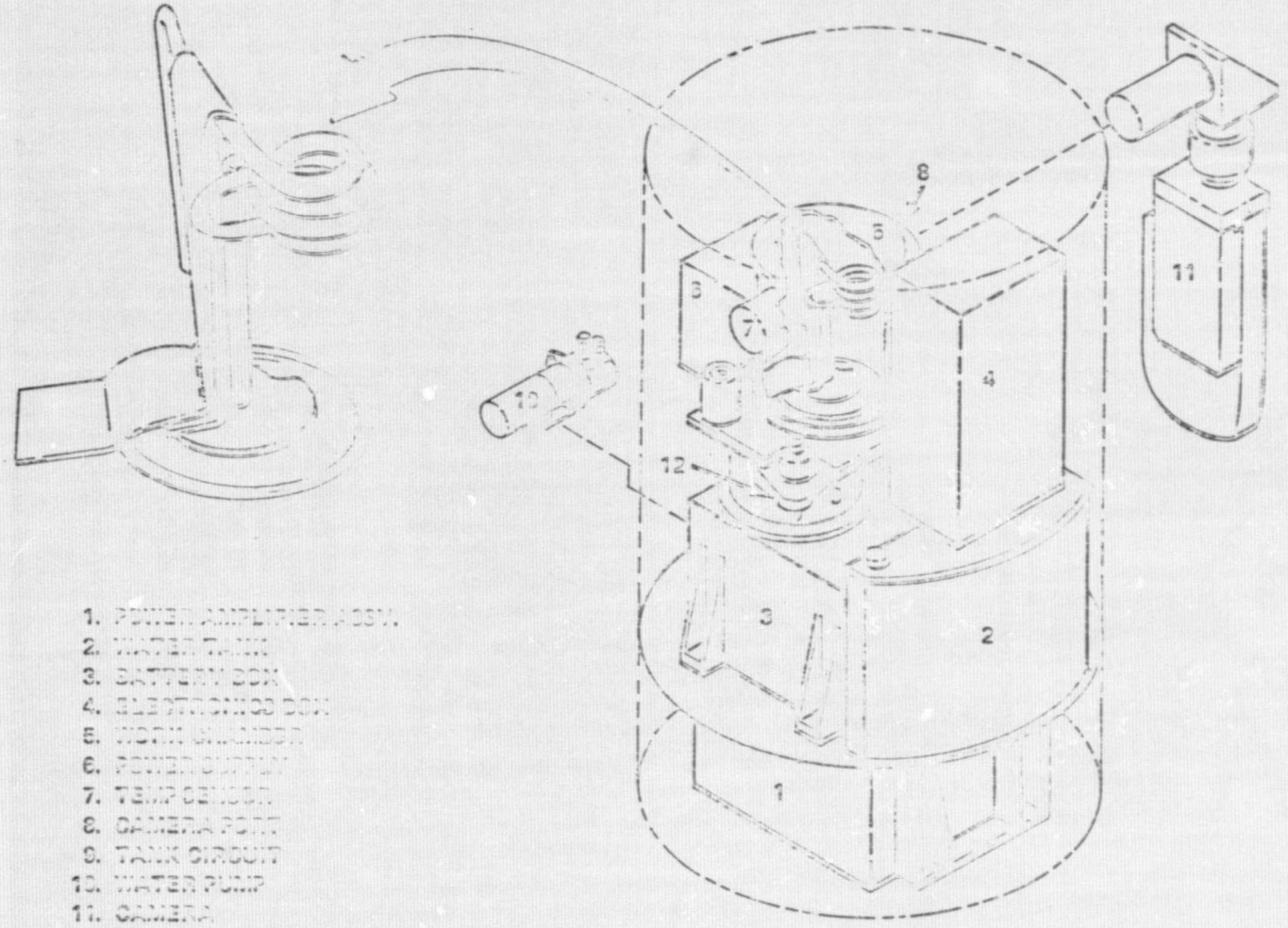

ORIGINAL PAGE IS
OF POOR QUALITY

Figure 1. Electromagnetic Levitation Furnace

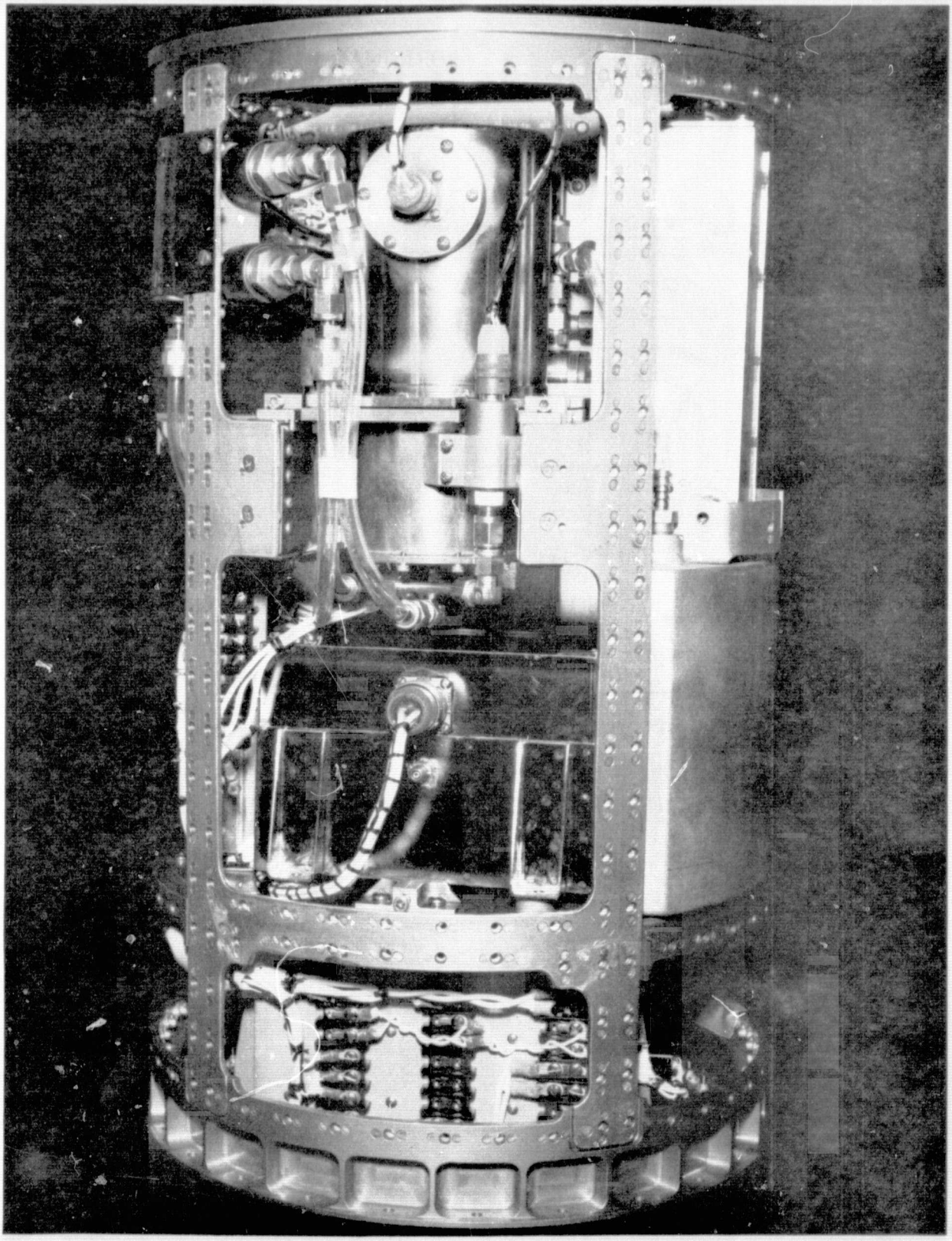

Figure 2. Electromagnetic Containerless Processing Package
(Outer skin removed)

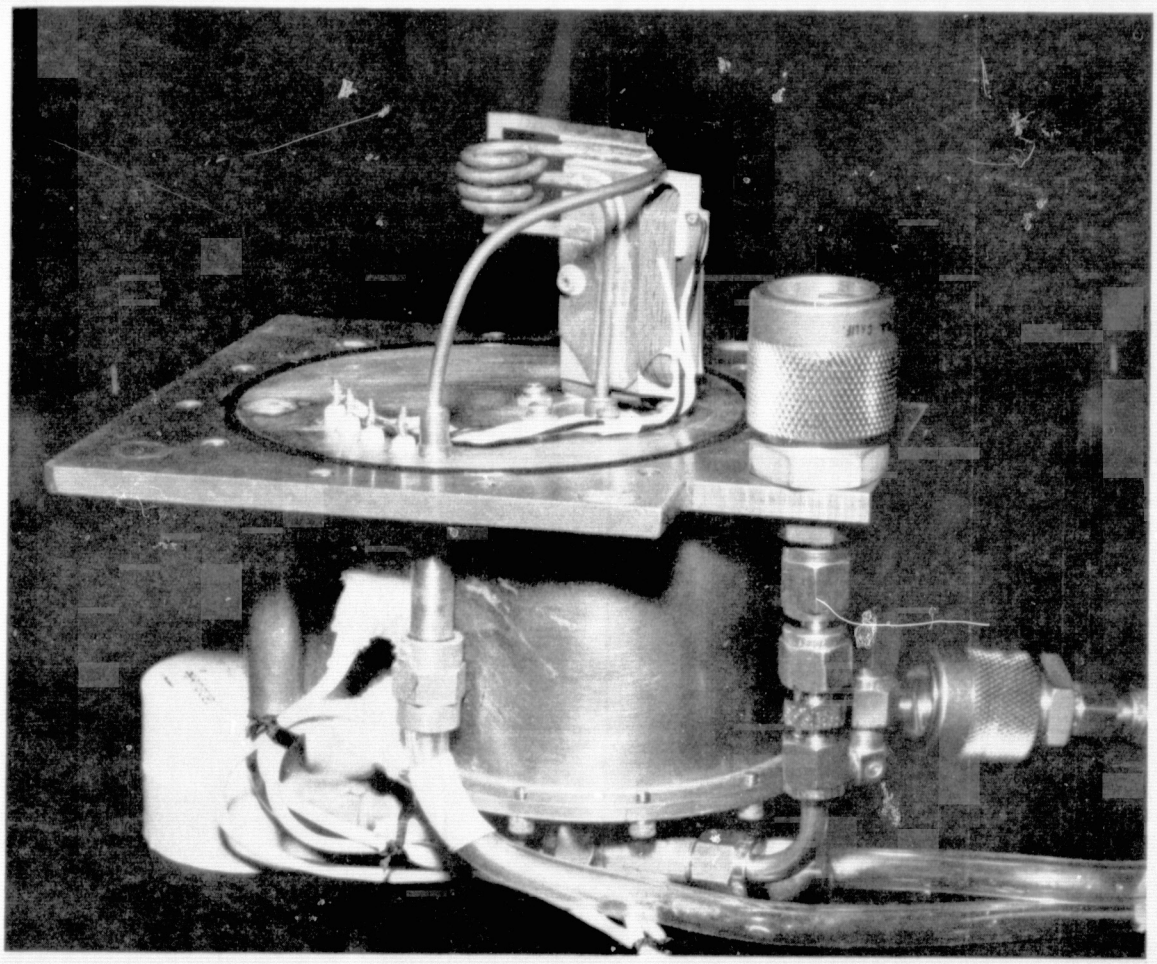

Figure 3. Work Coil and Matching Transformer

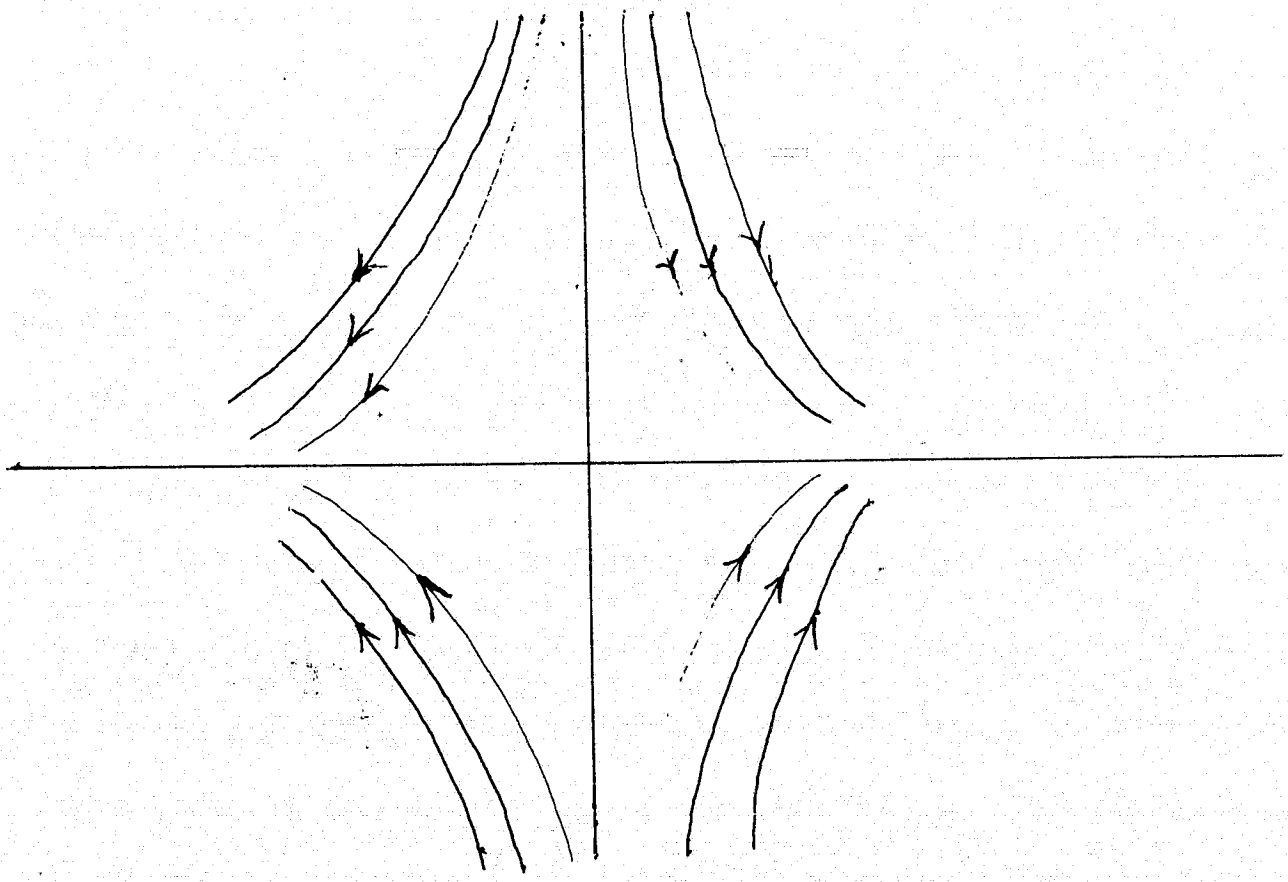

Figure 4. Field Lines Through Vertical Plane Section of Cusp Coil

2 parts per million of oxygen and 3 parts per million of water vapor and was dried by passing through a cold trap with liquid nitrogen as the coolant. Thus the water vapor and oxygen content of the gas was sufficiently low enough to prevent excessive oxidation of the specimen.

The experiment sequence is controlled by a timer, which switches full power on 50 seconds after launch of the sounding rocket, when weightlessness has been established, and then into a low powered mode about 160 seconds after launch, so that the specimen may solidify. The ECPP is fully automatic in operation when the timer sequence is initiated. A movie camera records the heating, melting, and solidification on film and a solid state, silicon detector records temperature data acting as a photometer. A full record of visual and temperature data is thus obtained. The performance and results of the flight experiment are described in Section 2.

SECTION 2
EXPERIMENT RESULTS

2.1 GROUND BASED EXPERIMENT RESULTS: BASIC METALLURGICAL STUDIES

Ground experiments performed were: (1) basic metallurgical studies and (2) ground based reference experiments. The basic metallurgical studies were performed in a hot wall furnace at KBI in commercial grade argon. With this furnace, the fastest cooling rate attained was 85°C per minute and cooling rates varied 45°C per minute to 85°C per minute. Beryllium, with compositions of 0.6% BeO, 1.5% BeO and 2% BeO by weight, was melted and solidified in this furnace. The 0.6% and 1.5% BeO alloys were high purity while the 2% BeO alloy was commercial purity. All of the alloys considered were prepared by hot isostatic pressing of powders and are standard KBI alloys.

Castings of these compositions were made of 0.922 centimeter diameter spheroidal specimens on a ceramic plaque (BeO) in the hot wall furnace. The basic metallurgical studies established: (1) a gravity effect on the BeO, showing agglomeration and settling, with the highest concentration of BeO at the bottom of each solidified specimen; (2) some retained BeO in the castings; (3) grain sizes of the order of 500 μm. The best castings with highest retained BeO and smallest grain size were with the 1.5% BeO by weight composition (HIP-50 alloy). Consequently this composition was selected to be the flight specimen composition. The agglomeration and settling observed were expected as this has been the previous result of terrestrial casting experiments. Retained oxide in the castings, however, was encouraging. As these experiments were preliminary to the ground based reference experiments, no detailed SEM analysis was made of the oxide distribution. Smaller grain sizes were found at the surfaces of these castings not in contact with the ceramic plaque, where the specimen cooled fastest by radiation. They were not small enough, however, to be of significance (less than 100 μm would be significant).

2.2 GROUND BASED REFERENCE EXPERIMENTS

The ground based reference experiments, performed in the General Electric Breadboard Facility constitute the best attempt, terrestrially,to duplicate the flight experiment. These experiments were performed with spheroidal specimens of the KBI HIP-50 alloy, approximately 0.922 centimeter in diameter at a pressure of 1 torr of research grade argon. The results of these experiments constitute the reference comparison between what can be achieved terrestrially and what can be achieved in the weightless environment of space, utilizing apparatus identical in essential aspects to the flight experiment apparatus.

Figure 5 shows the heating and cooling curve as observed by a disappearing filament pyrometer during the experiment. The specimen was sting mounted upon a tungsten-rhenium thermocouple. Temperature-time data was recorded from the breadboard pyrometer and the thermocouple. However, the breadboard pyrometer saturated before melting and the thermocouple data was not reliable due to poor contact between thermocouple and specimen. The disappearing filament pyrometer data is reliable however and, consequently, is the data presented.

2.2.1 GRAIN SIZE AND MORPHOLOGY

Preliminary experiments, conducted by induction melting in a glove box, small beryllium samples of a mass about equal to the flight specimen geometry, were characterized by microstructure evaluation. These specimens consisted of beryllium alloys with from 0.6% to 4.5% BeO by weight. The variables investigated were: (1) amount of BeO; (2) purity; (3) atmosphere (argon or vacuum); (4) dwell time in the molten state; (5) surface condition.

Heating and cooling rates were measured by optical pyrometry. The maximum cooling rate observed was 85°C/min. This is attributed to the relatively large mass of the furnace, susceptor, and crucible used. Superheat obtained was 70 to 100°C. Recalescence was observed on freezing of all melts with the exception of

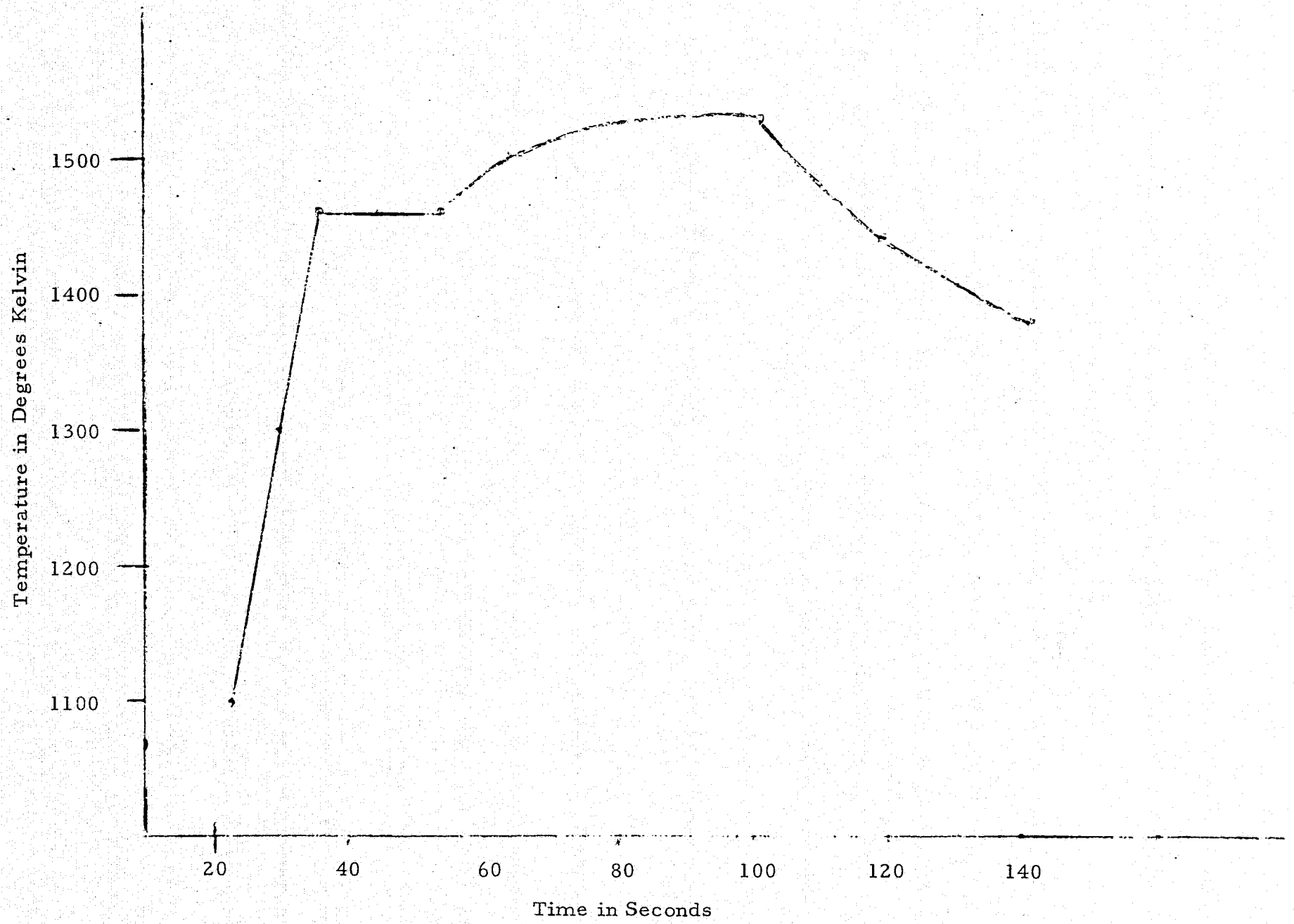

Figure 5. Time Temperature Curve for Ground Based Specimen #1

one at an apparent freezing temperature of 1200 to 1220°C. It was also observed that an approximately 2 μm BeO surface layer formed on all pieces regardless of purity and BeO content.

All specimens produced were large grained with average grain size of 500 μm. Voids were left where low melting impurity phases had melted out. Figure 6, taken with polarized light, shows the typical microstructure produced. Figure 7, taken in bright field, shows the voids present. From these studies, two compositions were selected and these were 0.6% BeO by weight and 1.5% BeO by weight. High purity specimens of these compositions were solidified in the above mentioned facility with cooling rates of about 65 to 80°C/minute and examined metallographically. The 1.5% BeO material showed the smallest grain size observed in the interior of the specimen. In contrast, the 0.6% BeO specimen showed a relatively fine grain size near the surface and extremely large grains in the interior. Therefore, the high purity 1.5% BeO material was chosen as the flight specimen material.

The flight and ground based experiments were conducted on material cut from a single pressing. Table I shows the mechanical properties based on an average of six tests, and Table II shows the grain size and chemistry. Two melts were made from the flight material using the above facility. Measured cooling rate for both melts was 60°C/min. Figure 8 shows the starting pressed microstructure and Figure 9 the microstructure after melting and solidification.

Two experimental melts were made in the General Electric breadboard facility, described above, using flight specimen material machined into 0.922 centimeter diameter spheres. Microstructure evaluation confirmed results of the previous work which was a relatively large grain size (though somewhat smaller than previously found) and development of porosity. Figure 10 (polarized light) and Figure 11 (bright field) show the typical grain size and shape and the voids respectively. These two experiments constituted the ground based reference experiments for comparison with the flight specimen microstructure.

Table I. Mechanical Properties of HIP-50 Alloy Billet, Billet Number 75044A

Grain Size (μm)	Ultimate Tensile Strength (KSI)	Yield Strength (KSI)	Elongation (%)
3.6	88.2	66.2	4.2
Based on Metallographic Measurements	Based on Average of 6 Tests	Based on Average of 6 Tests	Based on Average of 6 Tests

Table II. Chemical Purity of Billet Number 75044A (HIP-50 Alloy)

BeO	1.59% by Weight
C	390 ppm
Fe	450 ppm
Al	85 ppm
Si	33 ppm
Mg	21 ppm
Ni	88 ppm

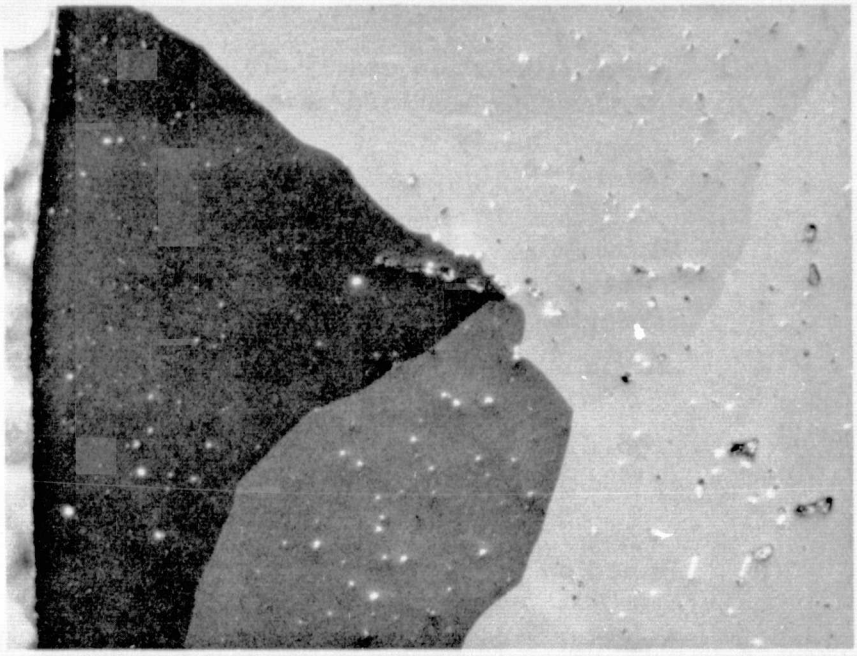

Figure 6. Typical microstructure produced from preliminary furnace experiments with HIP-50 alloy. Magnification is 100X. Taken with polarized light.

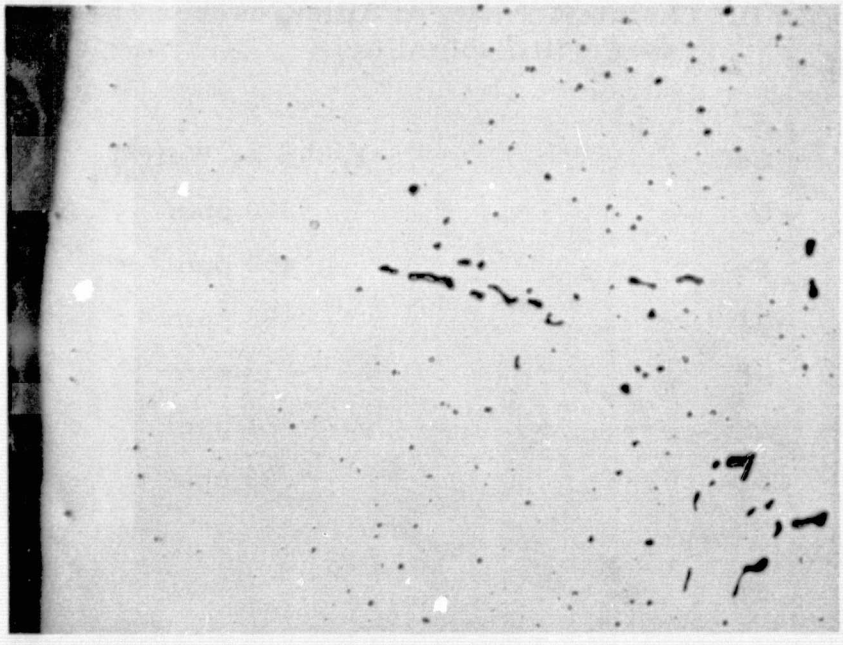

Figure 7. Bright field micrograph showing voids produced from preliminary furnace experiments with HIP-50 alloy.

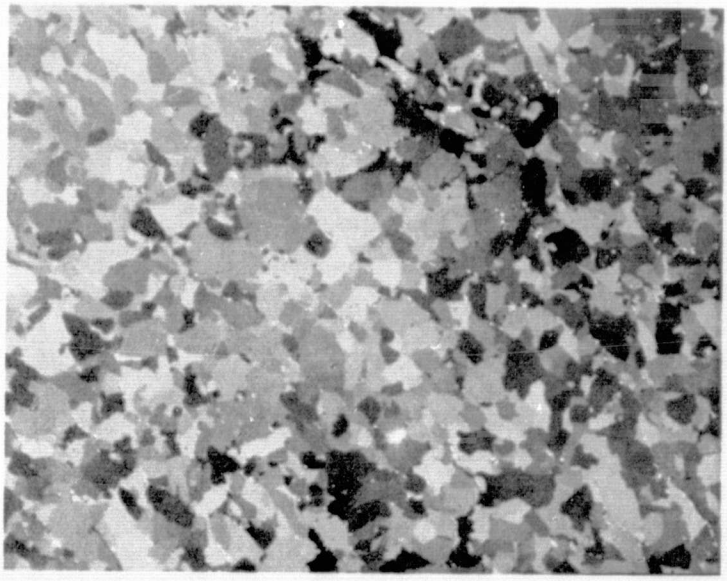

Figure 8. Starting pressed microstructure of HIP-50 alloy. Magnification is 800X.

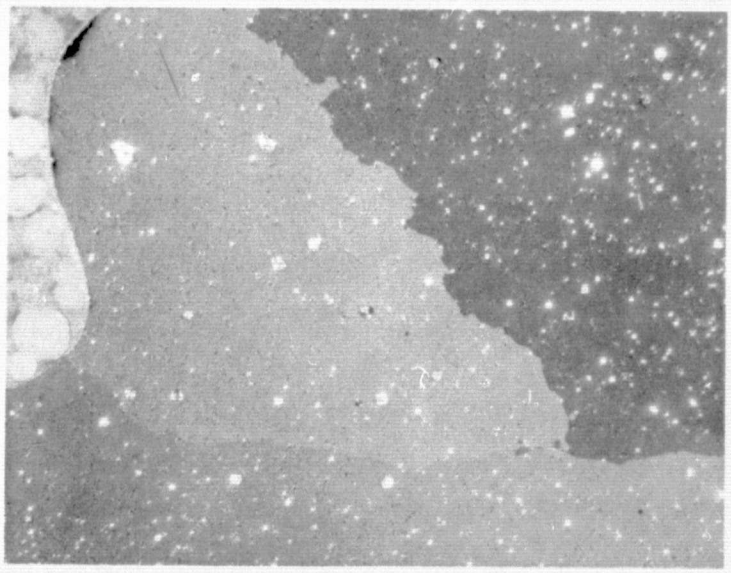

Figure 9. Microstructure produced from preliminary furnace experiment with HIP-50 alloy material cut from flight billet. Magnification is 100X. Taken with polarized light.

Figure 10. Microstructure produced from Ground Based Reference Experiment Number 2. Magnification is 100X. Taken with polarized light.

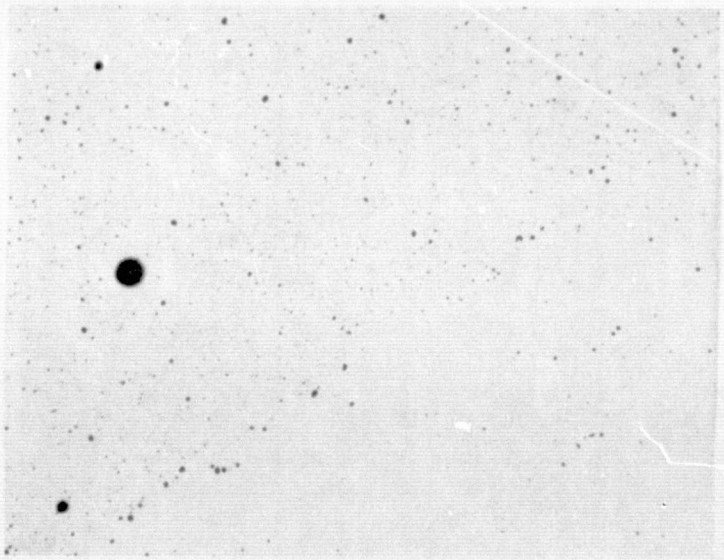

Figure 11. Bright field micrograph showing voids produced from Ground Based Reference Experiment Number 2. Magnification is 100X.

2.2.2 OXIDE PARTICLE DISTRIBUTIONS

Using scanning electron microscopy, the oxide particle distributions in the ground based reference specimens were characterized. Figure 12 is a montage of one of the specimens made up from 30X SEM micrographs after sectioning and metallographic preparation. It is the result of the experiment duplicating insofar as possible the flight experiment, terrestrially. It is observed that gross agglomeration and segregation of BeO have occurred. The dark areas are virtually cleared out of oxide whereas the white areas contain heavy agglomerations of oxide. Ground based reference specimen #2, which was melted and solidified at a slower rate, exhibits the same behavior showing gross agglomeration and segregation of BeO.

Detailed SEM studies to magnifications of 30,000X were made of the various regions comprising each specimen. An overlay was made for each specimen and the regions labeled alphabetically. Figures 13 through 16 show region A of Ground Based specimen #1 with magnifications 1000X, 3000X, 10,000X and 30,000X respectively. This is a region of moderately heavy oxide concentration, having a volume fraction of 2%, determined by Quantimet Analysis, for the 1000X micrograph. As can be seen in the 30,000X micrograph, the oxide networks are composed of agglomerates of small oxide particles ranging in size from 0.02 μm to 1.3 μm.

Figures 17 through 20 show region B of Ground Based specimen #1, with magnifications 1000X, 3000X, 10,000X and 30,000X respectively. This is a region almost devoid of oxide, having a volume fraction of 0.002% for the 1000X micrograph, determined by Quantimet Analysis. Figures 21 through 24 show region I of Ground Based specimen #1. This region is one of heavily agglomerated oxide. Ground Based reference specimen #2 is similarly made up of regions of heavy oxide agglomeration and regions devoid of such agglomeration.

Figures 25 and 26 are plots of the oxide volume fraction determined by Quantimet Analysis of identified regions of Ground Based reference specimen

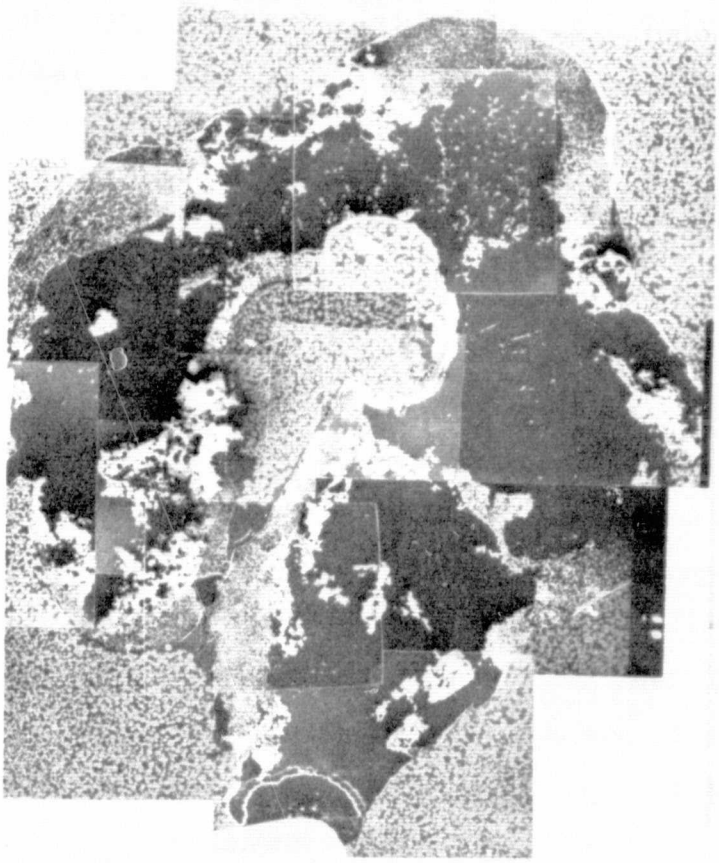

Figure 12. Montage of 30X SEM micrographs of Ground Based Reference Specimen No. 1, reduced to size for reproduction. White regions are heavily agglomerated regions. Dark areas are cleared out regions.

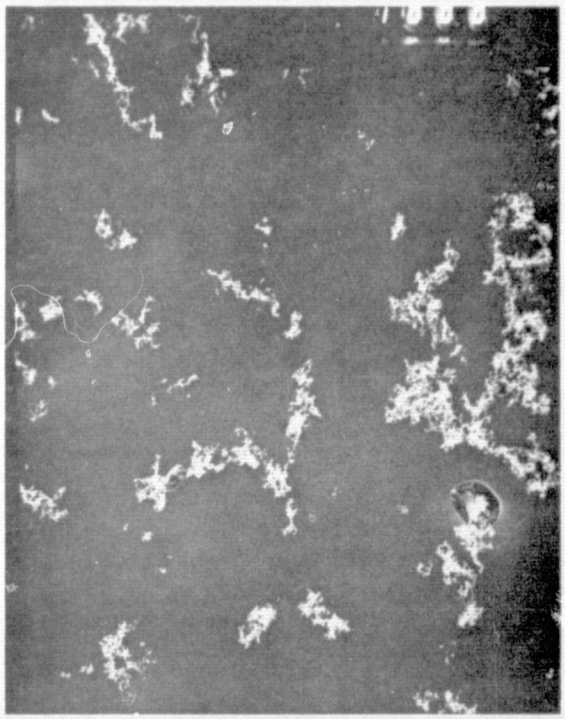

Figure 13

Figure 14

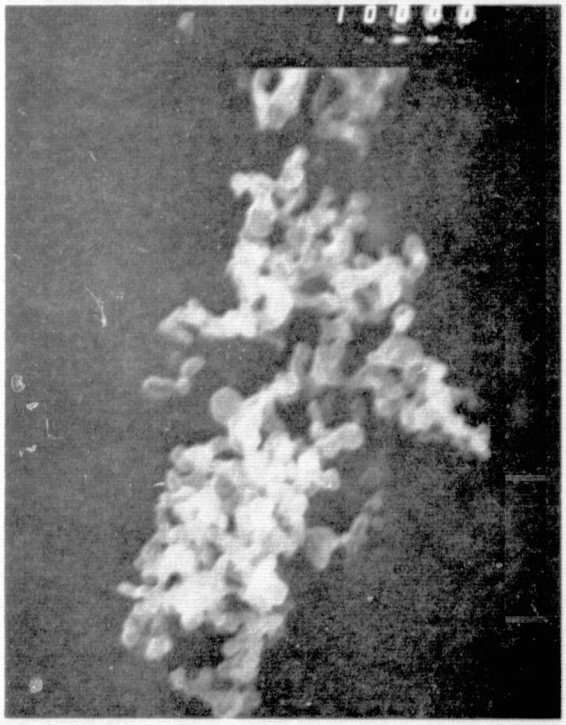

Figure 15

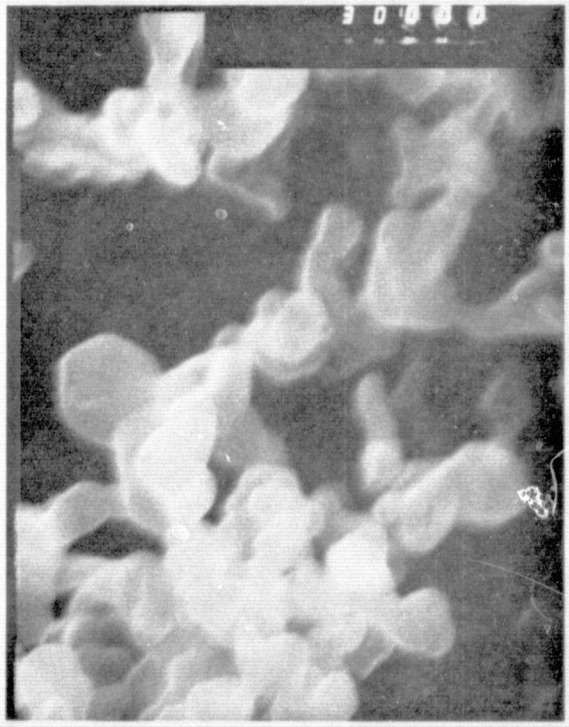

Figure 16

SEM micrographs of Region A from 1000X to 30,000X magnification. Region is not heavily agglomerated.

Figure 17

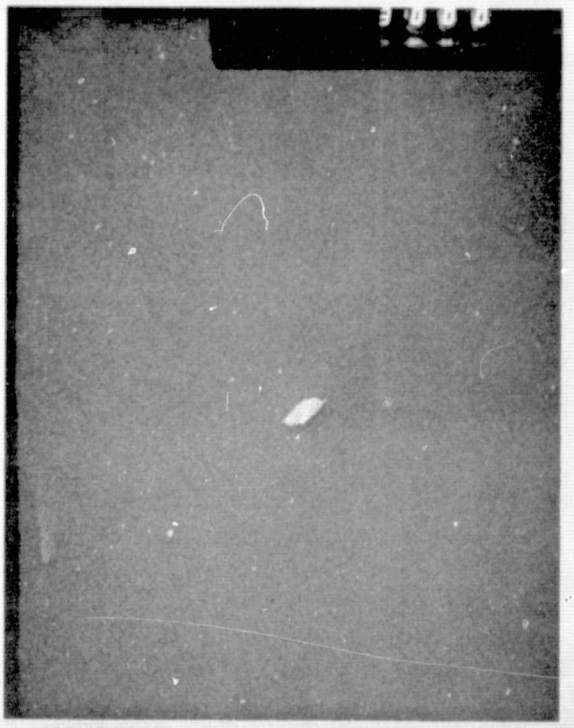

Figure 18

Figure 19

Figure 20

SEM micrographs of Region B from 1000X to 30,000X magnification. Region is virtually void of all oxide but one composite particle composed of oxide particles collected by collisions.

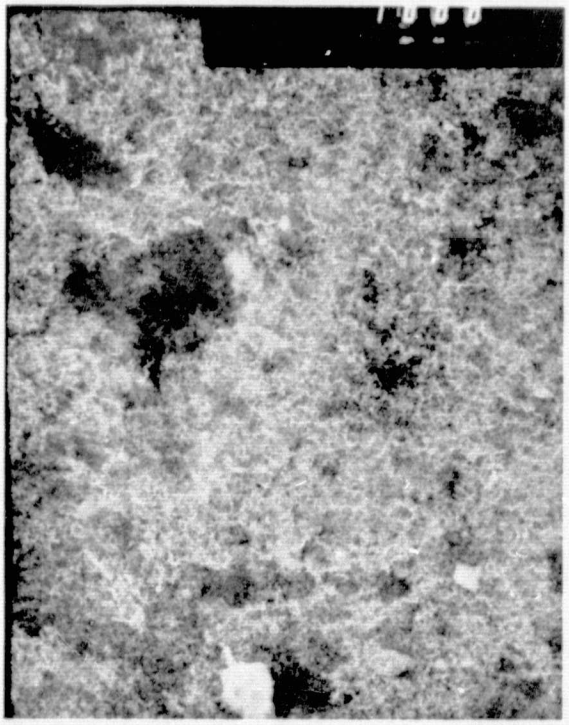

Figure 21

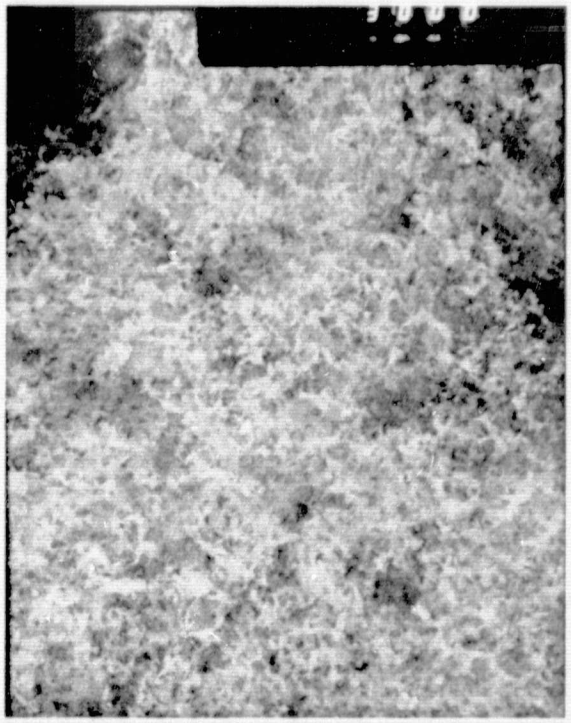

Figure 22

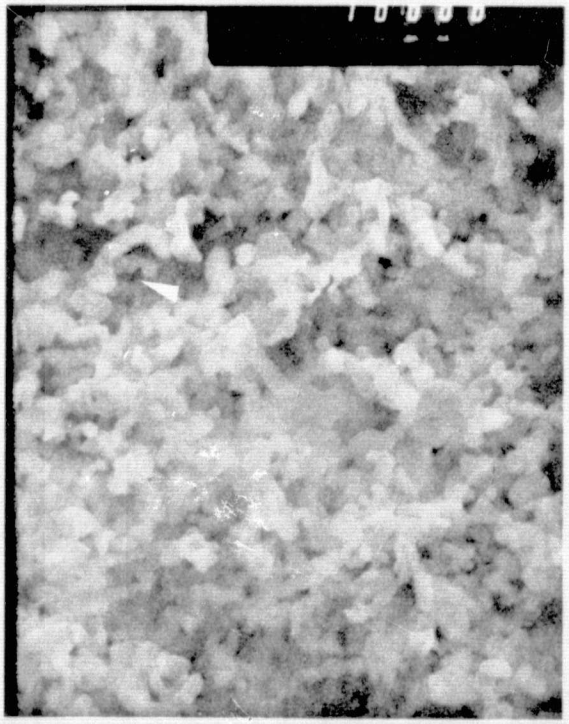

Figure 23

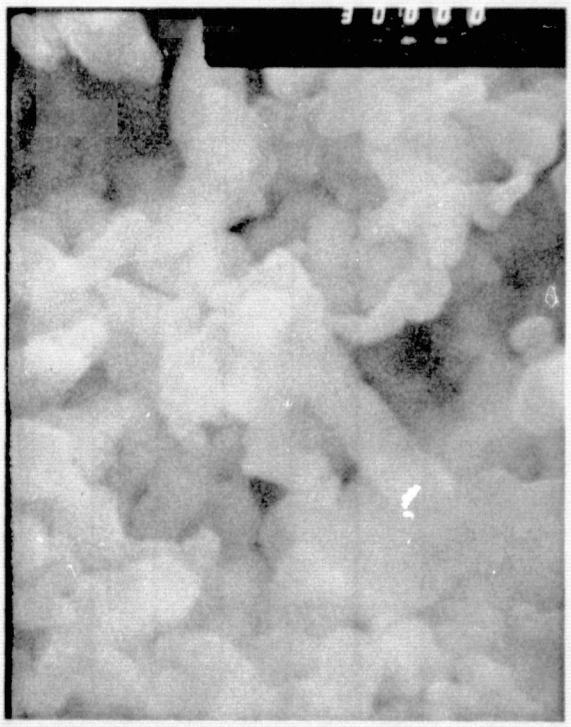

Figure 24

SEM micrographs of Region I from 1000X to 30,000X magnification
Heavy agglomerated region.

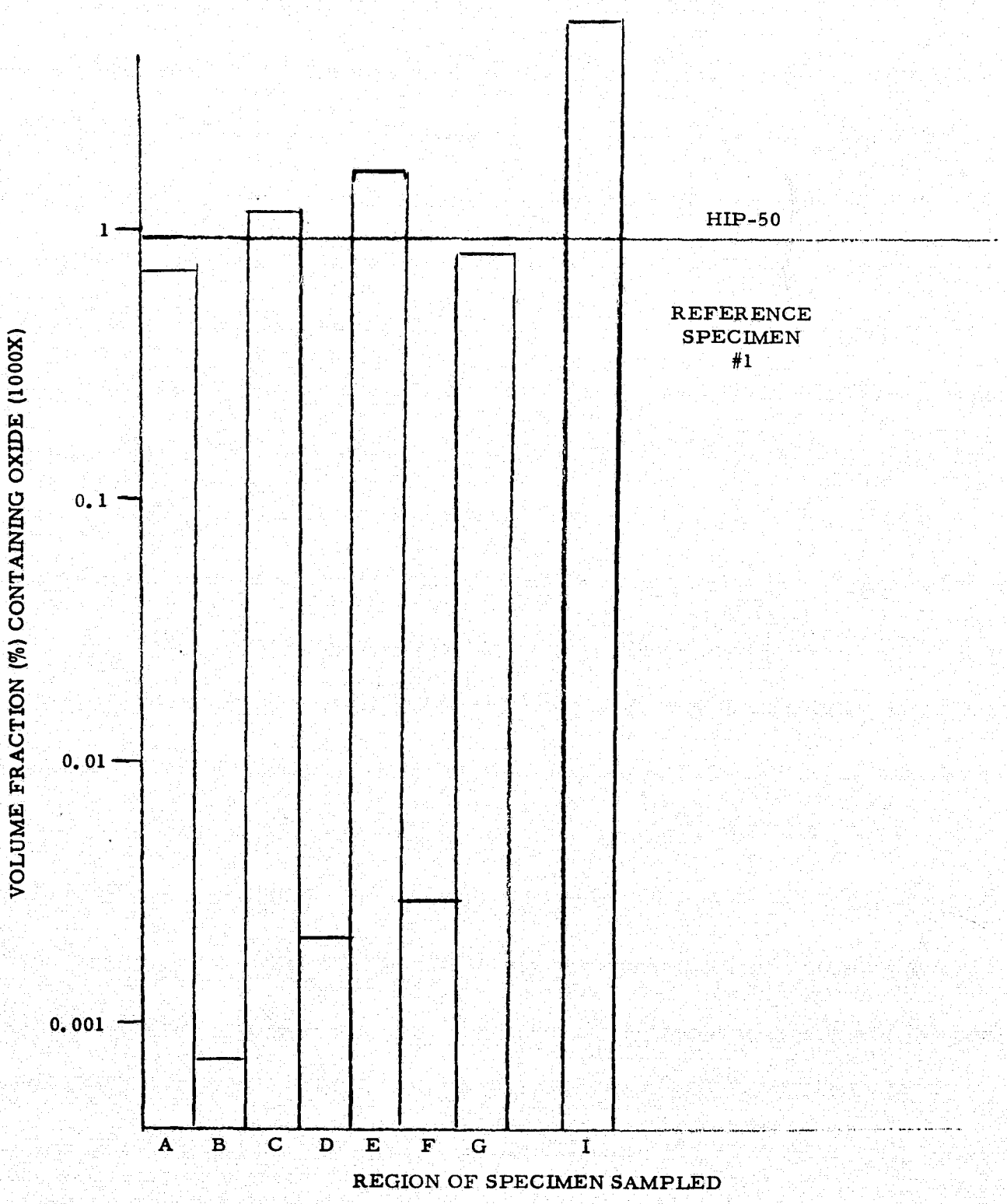

Figure 25. Oxide Volume Fraction produced from Quantimet Analysis of 1000X SEM micrographs for Ground Based Reference Specimen No. 1 after normalization to total volume fraction occupied by each type of BeO structure exhibited and to the initial distribution before melting.

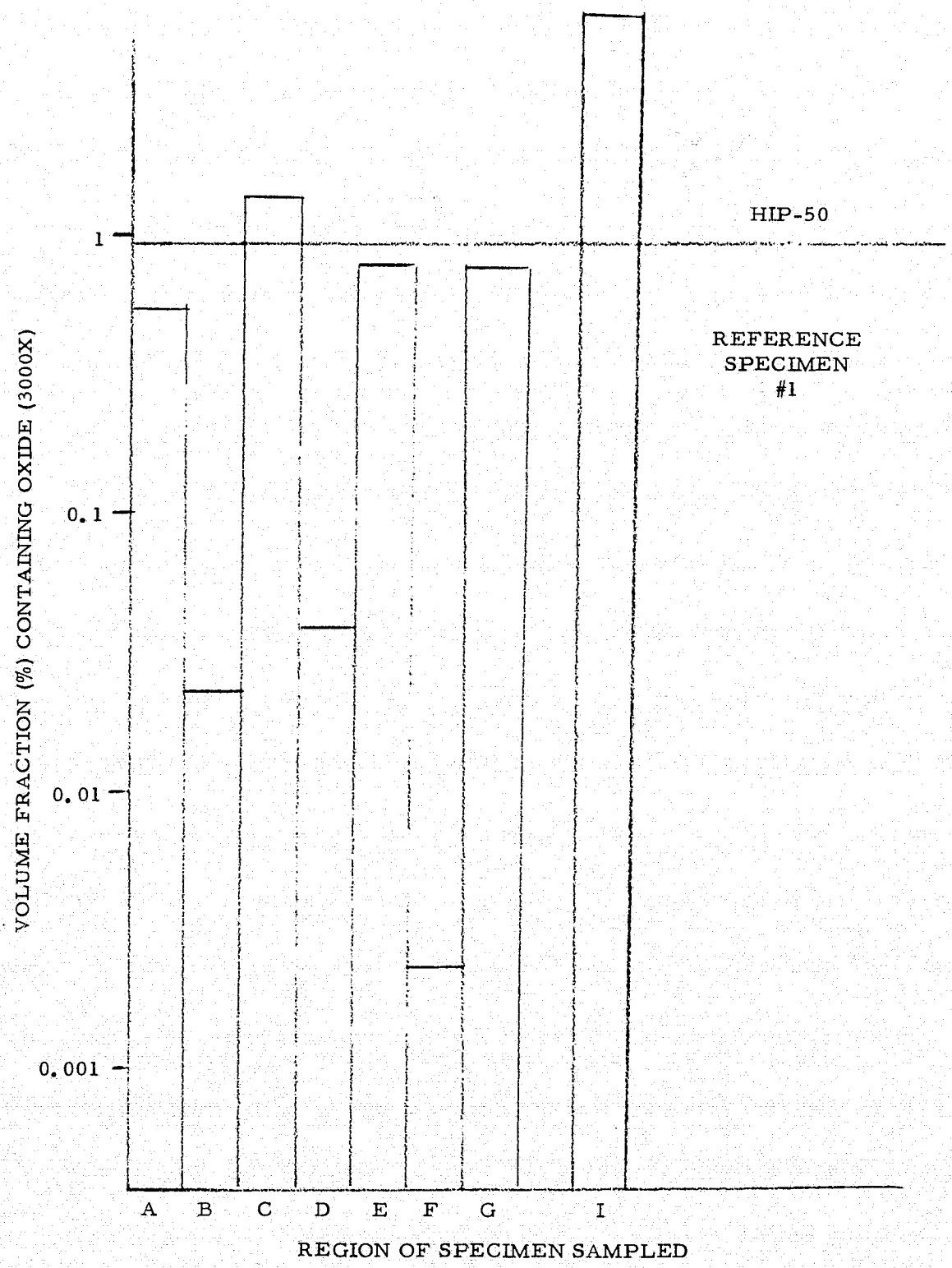

Figure 26. Oxide Volume Fraction produced from Quantimet Analysis of 3000X SEM micrographs for Ground Based Reference Specimen No. 1 after normalization to total volume fraction occupied by each type of BeO structure exhibited and to the initial distribution before melting.

#1 for 1000X and 3000X micrographs. Figures 27 and 28 are corresponding plots for Ground Based reference specimen #2. The fluctuations observed in volume fraction are indicative of the gross segregation of oxide observed in the terrestrial experiments. The differences are so large that four decade semilog paper were required to display the plots of volume fraction per region. The plots were normalized by volume fraction of region occupied by the type of BeO structure exhibited and to the initial BeO distribution before melting.

2.3 FLIGHT EXPERIMENT RESULTS

The flight experiment, flown on December 14, 1976 from White Sands Missile Range, performed the melting and solidification of a 0.922 centimeter diameter spheroidal specimen of HIP-50 beryllium alloy containing 1.5% BeO, under 18 psi of research grade argon, in the weightless environment of space. Table III shows the Major Event Record constructed from the telemetry records. Despite the failure of one of the power amplifiers 139.4 seconds after launch, the experiment operation proceeded as planned. The amplifier failure reduced the amount of superheating obtained. The major variable in the experiment was the weightless environment of space versus the terrestrial one gravity environment. The equipment operation is fully discussed in the final report for NASA Contract No. NAS8-30797, which was the hardware contract for construction and delivery to NASA of the ECPP. Only the pertinent aspects of equipment operation as regards to the experiment will be discussed herein.

Figure 29 is a macrograph of the specimen after solidification. As it was spheroidal before melting, there has been considerable shape change induced by the electromagnetic field configuration of the cusp coil. The specimen has assumed the "equatorial bulge" shape characteristic of the cusp field as discussed above. The stiff oxide layer prevented the specimen from assuming the spherical shape dictated by surface tension while molten when the power is turned down to initiate solidification. The cracks normal to the surface about the equatorial ridge are evident in this photograph and in the view shown in Figure 31. Figures

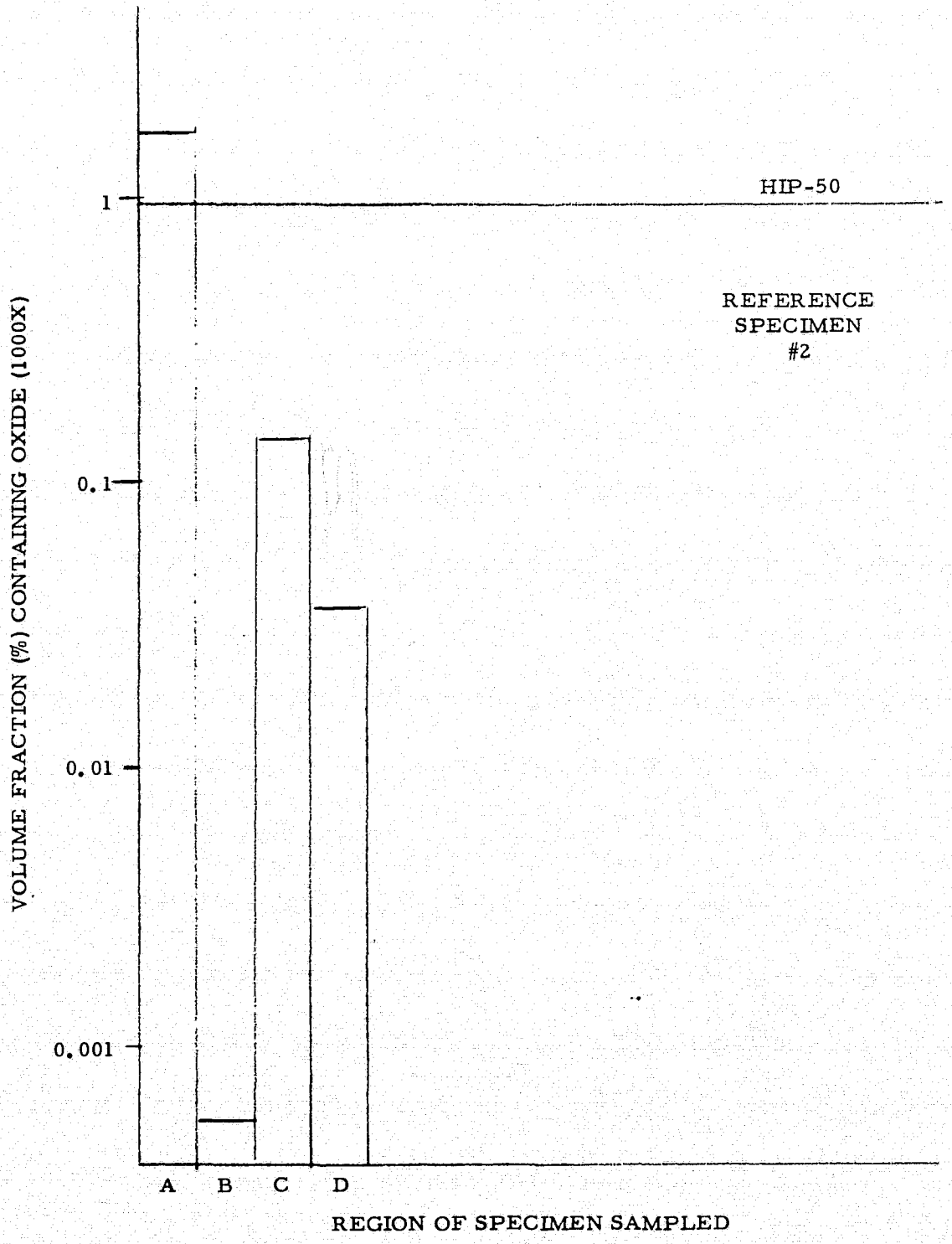

Figure 27. Oxide Volume Fraction produced from Quantimet Analysis of 1000X SEM micrographs for Ground Based Reference Specimen No. 2 after normalization to total volume fraction occupied by each type of BeO structure exhibited and to the initial distribution before melting.

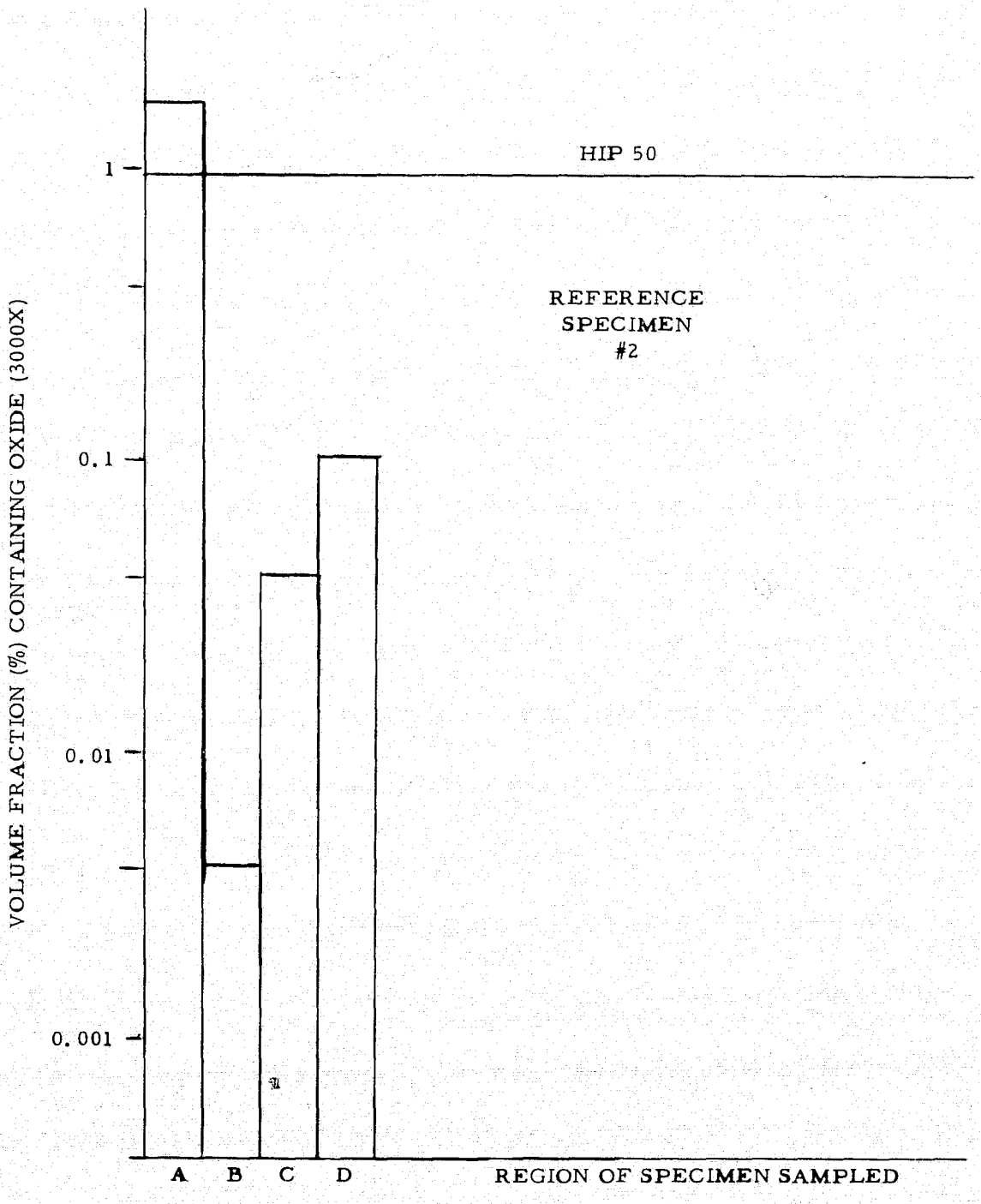

Figure 28. Oxide Volume Fraction produced from Quantimet Analysis of 3000X SEM micrographs for Ground Based Reference Specimen No. 2 after normalization to total volume fraction occupied by each type of BeO structure exhibited and to the initial distribution before melting.

Table III

Major Event Record

t	t -50.5	Event
0	0	Launch signal
50.5	0	Power on, specimen oscillations noted
85.9	35.4	First reading from solid state pyrometer
94	43.5	Solid state pyrometer reaches asymptotic reading nearly in saturation
121.3	70.8	Shape oscillation signal, completion of melting
139.4	88.9	Power reduction signal (33%), battery voltage increase
159.7	109.2	Initiation of low powered positioning mode
169	118.5	Attainment of low powered mode
261	210.5	Loss of telemetry signals

Figure 29. Specimen side view after recovery showing equatorial and polar bulge and surface penetration of shrinkage cavity

Figure 30. Specimen end view with shrinkage cavity

Figure 31. Oblique view from approximate angle of view by movie camera

30 and 31 are other views of the specimen. Possible explanations for the cracks are shrinkage or mechanical stresses supplied or a combination of the two.

Some of the external markings on the specimen apparent in Figures 30 and 31 may be indentations caused by the r.f. work coil. It is obvious from both the telemetry data and the movie record that the specimen did not contact the coil until after it had cooled below a dull red heat, except, possibly, at the instant of sudden shape change, at the moment of complete melting. The stiff oxide coating would have retained these markings. After the specimen had cooled below the self-luminescence temperature, during re-entry, forces between the specimen and the coil would not have been sufficient to cause such indentations, because the only available force would have been the inertia of the specimen which could have reached only about 70 grams under an assumed 70 g rocket impact.

During the experiment a record of the events were recorded on film by the motion picture camera provided and temperature-time data was recorded by telemetry signal from the flight pyrometer. Since the pyrometer temperature range was not sufficiently broad to include the superheat region, this portion of the record was not obtained. The measured melting interval and cooling curve will be discussed in a later section (Appendix A).

Telemetry and motion picture records show that the ECPP performed well the task of heating, melting, and positioning the specimen. This is discussed in detail in the NASA Contract No. NAS8-30797 final report. Aside from possible initial contact with the coil during the shape change upon melting, the specimen was not at any other time in contact with the coils and was stably positioned while molten. The experiment proceeded in all essential aspects as planned. The results are discussed below.

2.3.1 GRAIN SIZE AND MORPHOLOGY

In addition to the surface shape and markings described elsewhere in this report, macro study revealed the presence of a single shrink hole and many

surface cracks (Figure 29). Study of the microstructure (Figures 32 and 33) revealed a relatively large average grain size of 700 μm, porosity, and twinning and cracking. Although twinning can be induced during sectioning, it is most unusual that of the 17 large grain sized specimens sectioned, the flight specimen was the only one cracked and twinned.

With the very large grain size evident in the flight specimen, neither grain refinement of the beryllium nor retardation of grain growth was obtained, although detailed analysis of the dispersion of BeO (Section 2.3.2) showed that the BeO was unagglomerated and uniformly dispersed throughout the melt. This will be discussed in a later section. It must be concluded, in light of the above results, that the beryllia did not act to refine the grain structure and that minimum criterion (2b), that of improved microstructure through obtaining a fine grained casting (grain size less than 100 μm was not obtained. This is discussed below.

2.3.2 OXIDE PARTICLE DISTRIBUTION

Figure 34 is a montage of 30X scanning electron microscopy micrographs of the flight specimen after sectioning and metallographic preparation. It is evident that there are no cleared out regions devoid of oxide in the flight specimen. There is a darker band with less oxide present but Quantimet Analysis shows that there is still considerable oxide present in this region. Figures 35 to 38 show the oxide distribution at magnifications of 1000X, 3000X, 10,000X, 30,000X respectively in the lighter region and Figures 39 to 42 that in the darker region. Plots of the volume of oxide for different regions at 1000X and 3000X respectively obtained by Quantimet Analysis are shown in Figures 49 and 50. It is evident that even in the darker region, the oxide level is high although below that of the HIP-50 powder metallurgy starting material.

It can be seen that the oxide networks are made up of oxide particles in size ranging from 0.02 μm to 1.3 μm. Figures 43 to 46 show the oxide distribution typical to the HIP powder metallurgy material at magnifications 1000X, 3000X, 10,000X and 30,000X respectively. It is evident that the oxide networks in the

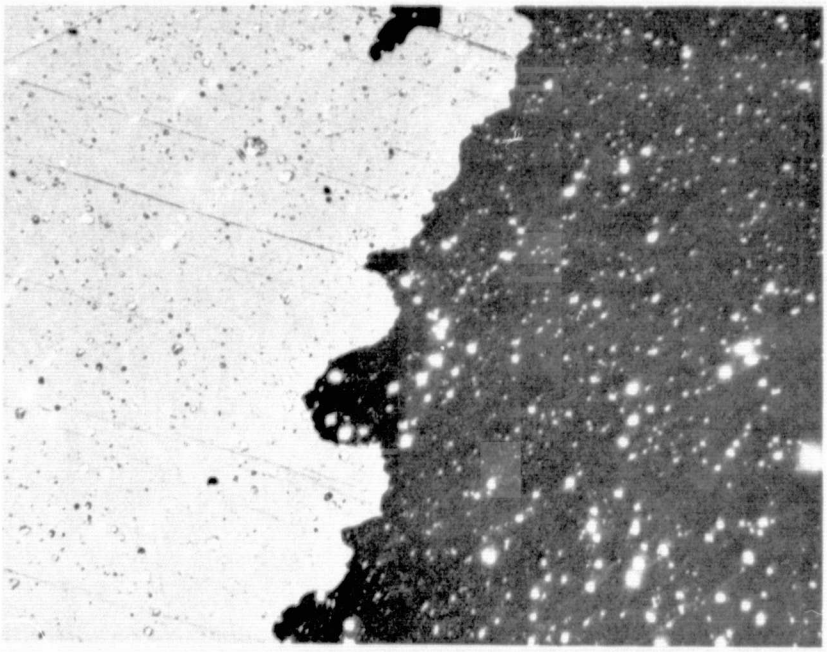

Figure 32. Typical microstructure exhibited in flight specimen. Taken with polarized light.

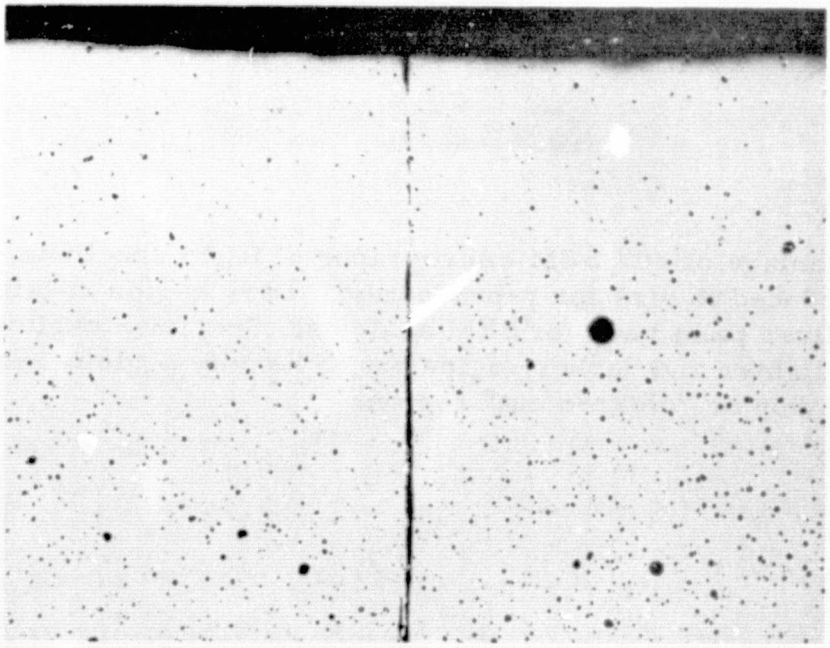

Figure 33. Bright field micrograph of flight specimen showing a crack running in from surface and voids produced. Magnification 100X.

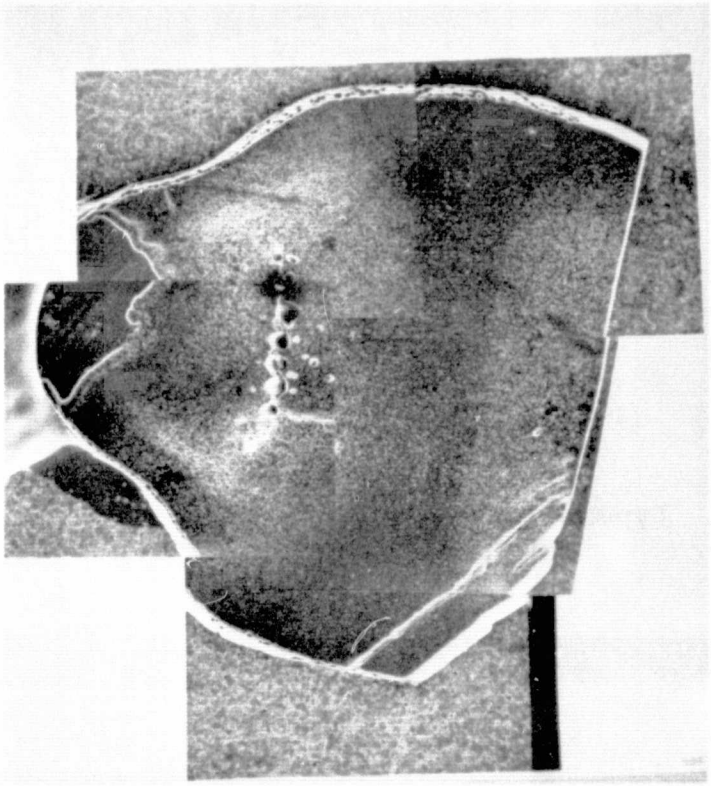

Figure 34. Montage of 30X SEM micrographs of flight specimen, reduced to size for reproduction. Dark region at left is silver paint used for SEM analysis. Specimen exhibits a lighter and darker region but no heavily agglomerated region or "cleared out" region.

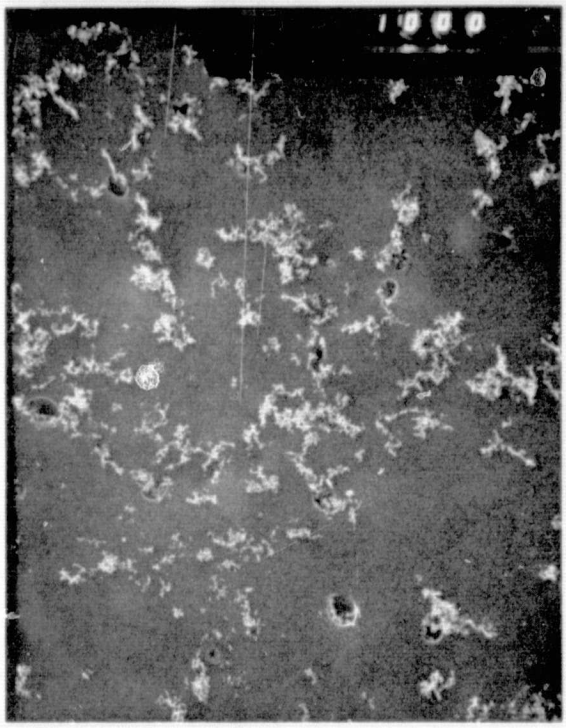

Figure 35

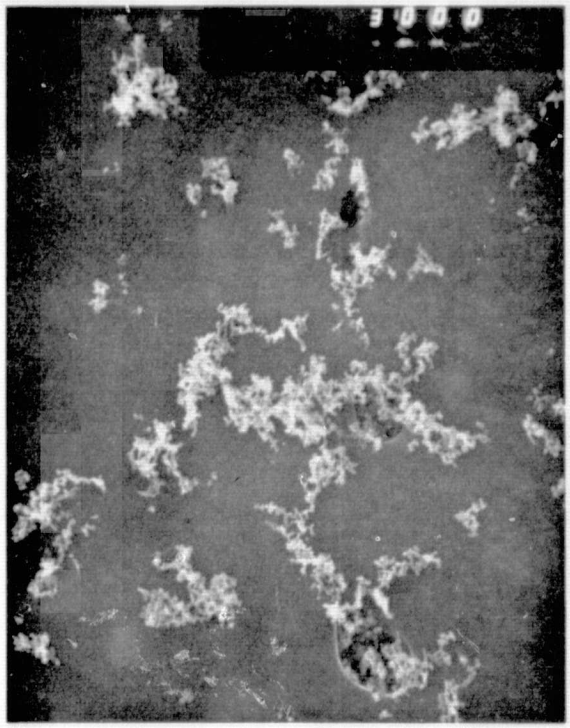

Figure 36

Figure 37

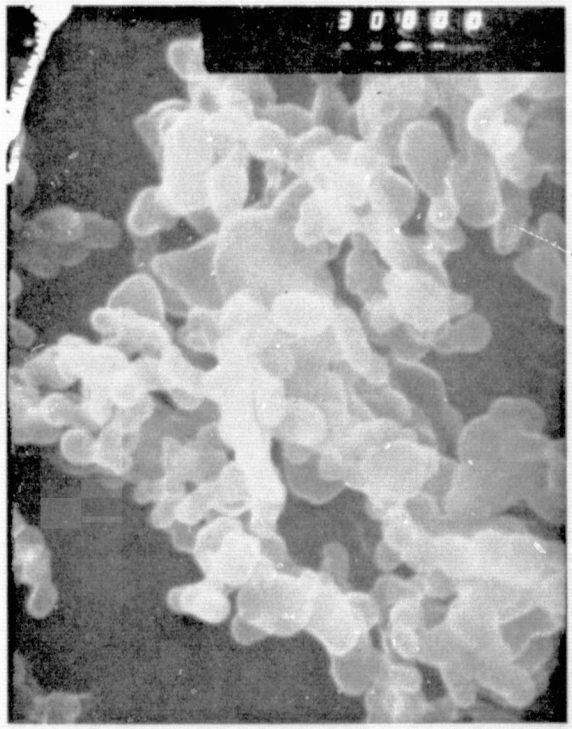

Figure 38

SEM micrographs of lighter region of flight specimen
from 1000X to 30, 000X

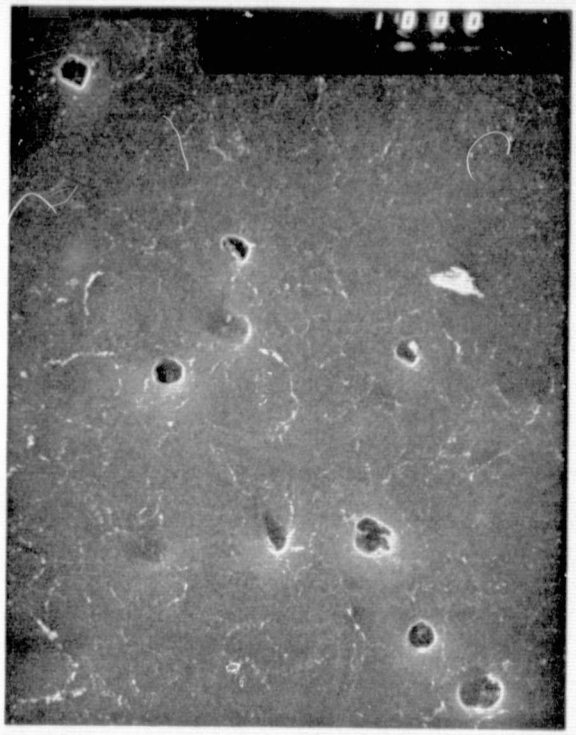

Figure 39

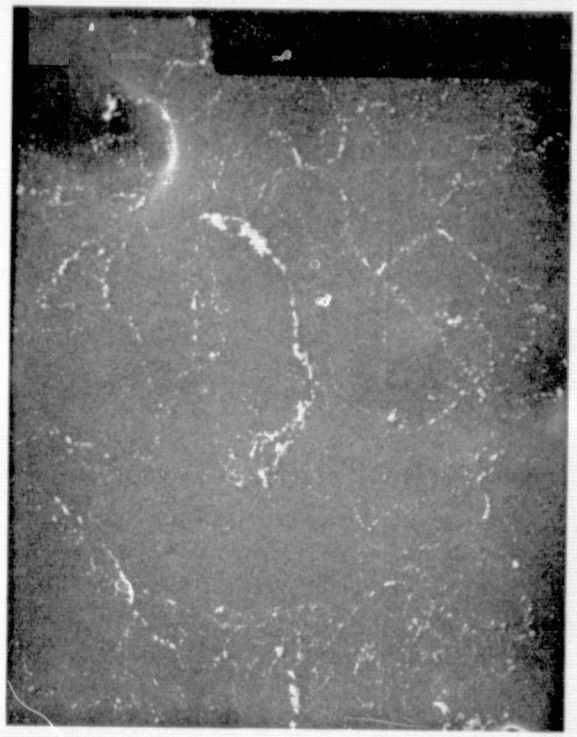

Figure 40

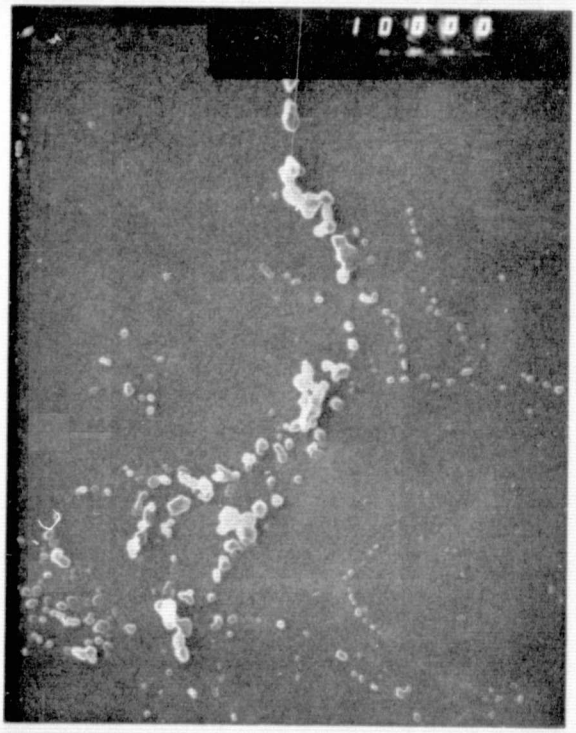

Figure 41

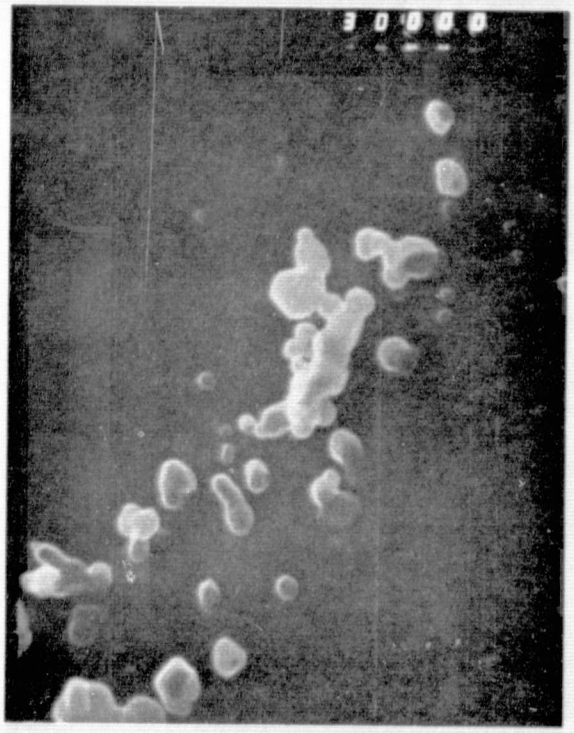

Figure 42

SEM micrographs of darker region of flight specimen
from 1000X to 30,000X

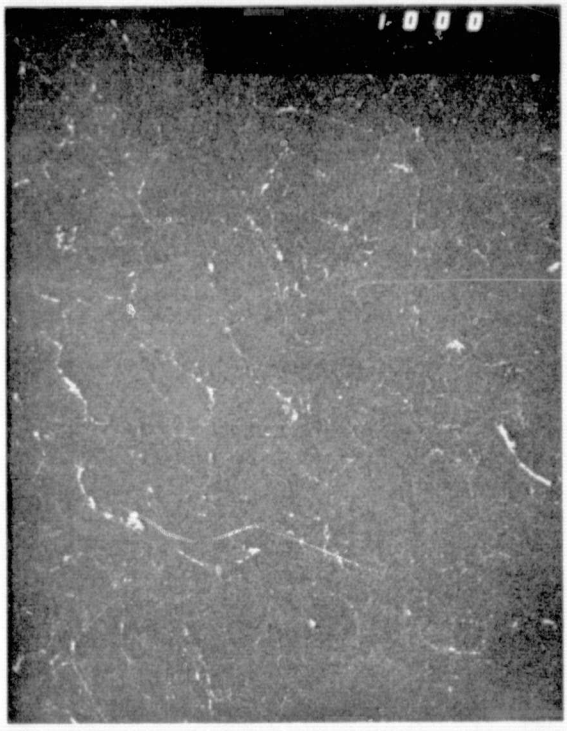

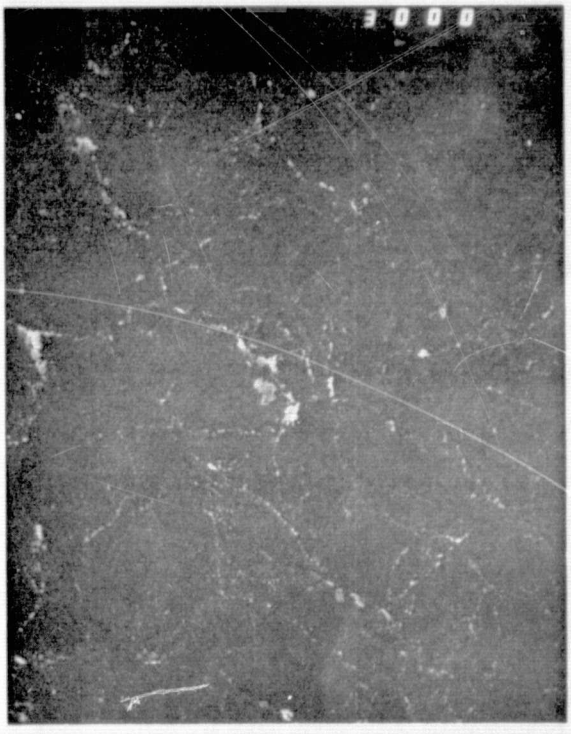

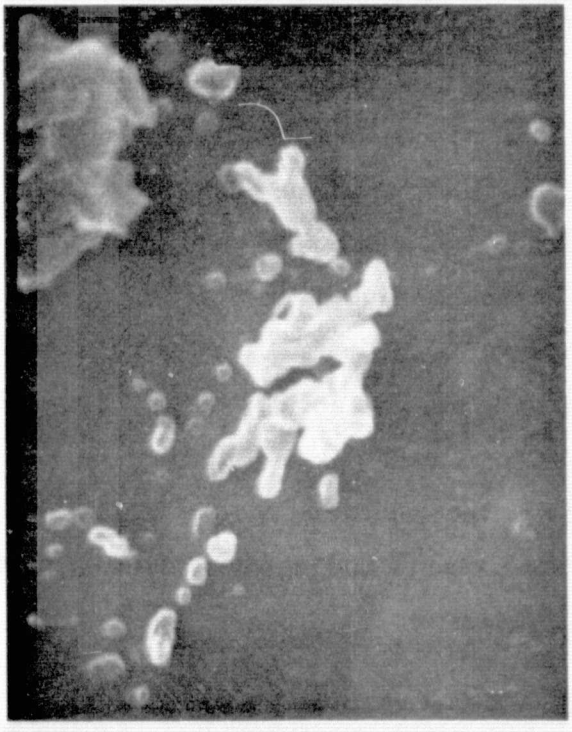

Figure 45

Figure 46

SEM micrographs of initial oxide distribution before melting in HIP-50 alloy from 1000X to 30,000X

darker region of the flight specimen are most like those of the starting material, even though the flight specimen is coarse grained and the powder metallurgy material very fine grained. This is a very encouraging result as in this region, the oxide network structure did not change much, even though the specimen was molten. It will be observed that the volume fraction results obtained by Quantimet could be plotted on linear graph paper. There are no cleared out areas devoid of oxide. There are also no very white areas with heavily agglomerated oxide. In every region of the specimen there is appreciable oxide content and no gross agglomeration and separation are evident.

It was determined by microprobe analysis (SEM microprobe attachment) that silver flakes are present in the specimen surface oxide coating and there are silver inclusions on the sectioned surface of the flight specimen. These are shown in Figures 47 and 48 respectively. It was determined that the silver inclusions were a polishing artifact on the following basis: (1) The silver particles are sharp faceted. Had they been present in the molten beryllium, they would have either gone into solution in the beryllium or been spherodized; (2) a transverse section to the section where they are present did not reveal any silver inclusions in the specimen. The silver on the specimen surface oxide coating is not a polishing artifact but also had to be deposited after solidification. Otherwise it would have dissolved in the beryllium or spherodized on the surface (silver melts at 961^{o}C). Most of the solder used in the ECPP contains silver and, while still hot but solid, the specimen rattled around in the coils and the ECPP was shaken considerably during the re-entry and impact with the ground. The silver in the form of flakes was deposited on the specimen during this period and was not present during the experiment and is believed to have had no effect on the experiment.

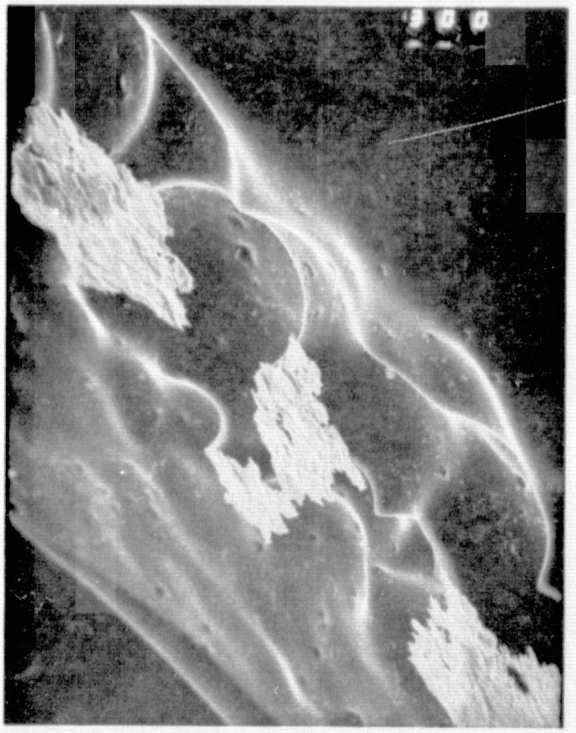

Figure 47. Silver flakes on surface oxide coating of specimen.
Magnification 300X

Figure 48. Silver inclusions in specimen.
Magnification 2000X.

SECTION 3
ANALYSIS OF EXPERIMENTAL RESULTS

Examination and comparison with each other of the Quantimet plots of volume fraction of BeO for different regions of the ground based specimens and the flight specimen (Figures 27, 28, 29, 30, 49, 50) show the flight specimen is much more uniform in oxide distribution from the ground based specimens. The flight specimen has no regions devoid of oxide or regions filled with oxide as has both ground based reference specimens. The reason for this is postulated to be the weightless environment of space, where the g-level has been reduced to 10^{-4} g, during the melting and solidification. The Stokes Collisions (see Appendix B) are reduced for a given distribution of particle sizes directly in proportion to the reduction in g-level and the separation time is inversely proportional to the g-level. Hence on the basis of Stokes Collisions alone, the time for agglomeration and separation to occur should be greatly extended in the weightless environment of space.

Collisions due to fluid motion (Gradient Collisions) which may arise due to stirring, gravity driven convection, or Marangoni convection (surface tension driven convection) act to speed up agglomeration and separation. In the weightless environment of space gravity driven convection is greatly reduced but the other sources of fluid motion are not. What this experiment indicates, is that the major mechanism for agglomeration and separation of BeO from the melt may be Stokes Collisions as the stirring forces and Marangoni convection are essentially the same in the ground based and flight experiments.

The coarse grain size of the ground based reference specimen and the flight specimen indicate that the BeO present did not act as a grain refining agent for beryllium or that after solidification it did not prevent excessive grain growth while still at high temperatures. Returning to the criteria stated in 1.0 for a good grain refining agent, possible reasons for this are either the particles are not stable in the melt, do not possess a maximum of surface area or do not

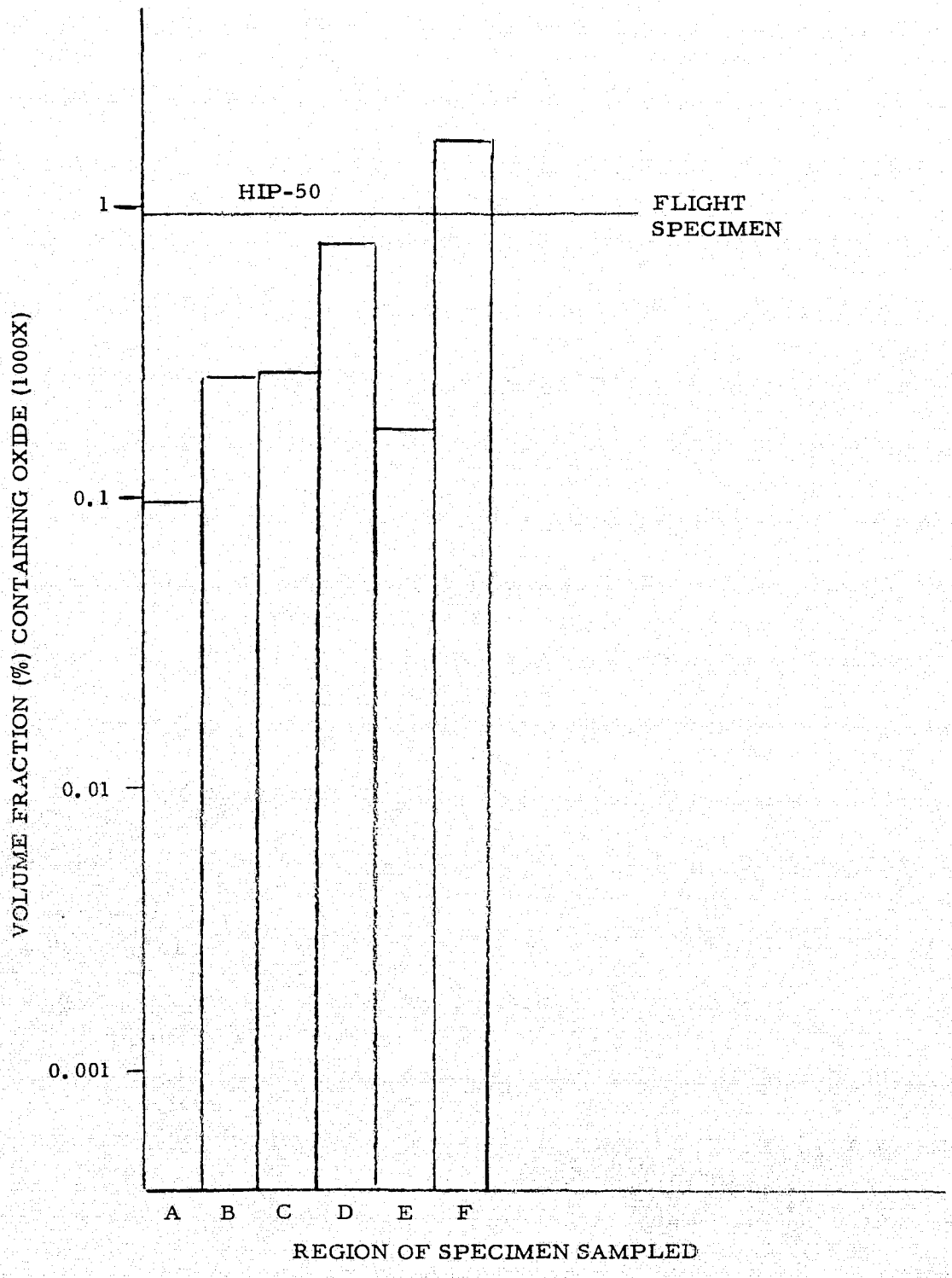

Figure 49. Oxide Volume Fraction produced from Quantimet Analysis of 1000X SEM micrographs for Flight Specimen No. 1 after normalization to total volume fraction occupied by each type of BeO structure exhibited and to the initial distribution before melting.

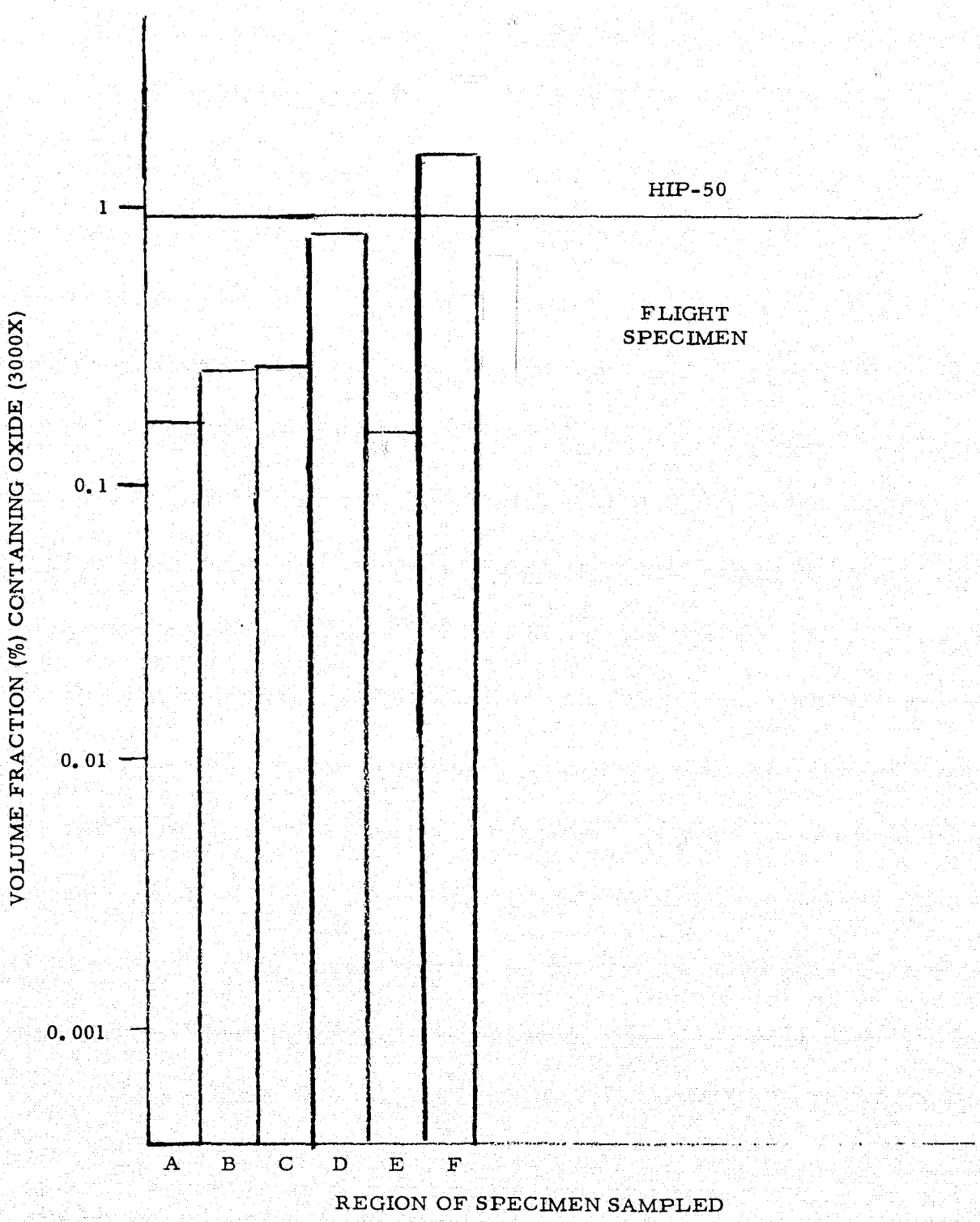

Figure 50. Oxide Volume Fraction produced from Quantimet Analysis of 3000X SEM micrographs for Flight Specimen No. 1 after normalization to total volume fraction occupied by each type of BeO structure exhibited and to the initial distribution before melting.

have optimum surface character. Examination of the oxide networks in the HIP-50 alloy (Figures 43 to 46) shows that even before melting, the particles tend to be rounded and without sharp facets. It may be possible that as a result of the long molten dwell, the particles change their surface character as well and become inactive as sites for heterogeneous nucleation but this could not be observed at 30,000X. An optimum surface character (Ref. 1) might be a rough or pitted surface.

Prevention of excessive grain growth after solidification, while still near the melting point, depends greatly on the oxide particle size. While the HIP-50 alloy has stability against grain growth temperature almost to the melting point of beryllium, further agglomeration while in the molten state, even in the weightless environment could lower the stability temperature significantly. Work reported (Ref. 2) indicates that the finest particle size attainable is required to prevent grain growth at temperatures near the melting point (0.065 μm median particle size). Attention must be given to this aspect in future work.

SECTION 4
CONCLUSIONS

The experiment results show that it is feasible to obtain a uniform dispersion of BeO in a beryllium casting in the weightless environment of space. This is a new material, which, to our knowledge, has not been produced in the terrestrial environment. It is of interest both scientific and technological. In terms of the minimum criteria for success, criterion (1) satisfactory melting and solidification and (2a) improved cast microstructure - presence of dispersed oxide phase were met. Criterion (2b), improved cast microstructure - fine grain size, was not met. Criterion (3),enhanced service properties, has not been met as yet because of failure to achieve criterion (2b).

As a step forward in producing cast beryllium with improved service properties, the material produced delineates an approach to be followed for further research into the action of BeO as a grain refining agent for beryllium. This approach is: (1) to utilize beryllium starting material with non-spherodized BeO particles dispersed throughout. This can be achieved by elimination of the final step in the production of HIP-50, the high temperature dwell at 1950°F (1038°C); and (2) to dwell for a much shorter time while molten during the experiment. Additionally, the experiment should be performed at very low pressure (1 torr) to reduce the observed 2 to 5% porosity in the casting.

If a subsequent experiment with BeO particles that are not spherodized is performed and grain refinement does not result, then serious questions are raised about the ability of BeO to act as a grain refining agent. In that event, the weightless environment of space is ideal to test the potential of several other additions as grain refiners. One such addition is titanium, which forms a beryllide in the melt. Attempts to utilize titanium as a grain refining agent may have failed terrestrially also because of agglomeration and separation of the beryllide from the melt. Another such addition would be tungsten.

Failure to achieve grain refinement with a particular agent, chosen on the basis of lattice disregistry may mean that other factors are of overriding consideration such as surface area or surface character or grain growth after solidification. If grain growth is so rapid that grain refinement is not achieved, then the number of nucleating particles becomes of great importance rather than surface area or surface character. In that case, so many particles may be required that mechanical properties may be greatly impaired even with grain refinement. Testing of all of these factors is important to explaining why or why not an agent is successful as a grain refiner. Such experiments conducted in the weightless environment are the only practical methods of testing these hypotheses, as terrestrially agglomeration and separation are encountered.

References

1. Flemings, M. C., "Solidification Processing," McGraw Hill, Inc., 1974.

2. Webster, D., Crooks, D. D., and Vidoz, A. E., "The Effect of Oxide Dispersions on the Recrystallization of Beryllium," Met. Trans. 4 (1973), 2841.

3. Lindborg, U., Torsell, K., "A Collision Model for the Growth and Separation of Deoxidation Products," Trans. Met. Soc. AIME, 242 (1968), 94.

4. Gelles, S. H. and Malik, R. K., "Process Development for Producing Fine-Grain Castings in Space," NASA Contract NAS8-29626, 1975.

APPENDIX A

THERMAL ANALYSIS

Although the flight pyrometer was in saturation during the melting and molten dwell, enough data are obtained from the telemetry records and the cooling curve to reconstruct the heating, melting, and cooling profile. The flight record of events is presented in Table III. The heating and cooling curves obtained from the flight pyrometer are shown in Figures 51 and 52. From analysis of the data available, the temperature-time curve shown in Figure 53 was constructed. The solidification time after power down was 28 + 5, - 0 seconds.

A computer model of the solidification of the beryllium specimen was exercised to determine whether or not the assumptions made about how the beryllium specimen solidified were reasonable. This model assumes that the specimen solidifies inward from the surface, losing heat at the surface by radiation. The remaining liquid at any time is assumed to be well mixed and at the melting temperature. Outputs from the program are: (1) the advance of the solidification front in time and (2) the decrease in surface temperature with time. The program can treat a sphere, a cylinder, or a slab. As the remaining liquid is isothermally at the melting temperature, heat is extracted through the solid crust to the surface, where it is lost. Figures 54 through 59 show the results of calculations for a sphere of 0.922 cm diameter, a cylinder of 0.922 cm diameter, and a slab of 0.922 cm thickness.

Comparisons with the experimental curve shown in Figure 53 show that the calculated time that agrees closest is for the spherical geometry, but the shape of the cooling curve is closest to that of the slab. The calculated solidification time for the sphere is 31 seconds, which is within the error of determination of the time for solidification experimentally. As the shape of the specimen is spheroidal with an equatorial bulge, its geometry is closest

to that of the sphere and so the agreement in solidification time is reasonable. The location of the shrinkage cavity shows that the specimen did not solidify symmetrically as is assumed for the calculation. This is the hypothesized reason for the disagreement in the shape of the cooling curve, which is closest to that of the slab geometry.

As the computer model uses the known values of thermal conductivity, latent heat of fusion, and emissivity for molten beryllium (emissivity for oxidized beryllium), the results indicate that it might be possible to extract thermodynamic data from solidification curves of levitated metals if the shape of the specimen and the details of solidification are known. This might be accomplished through the use of an imaging array pyrometer to simultaneously display the specimen and follow the solidification front.

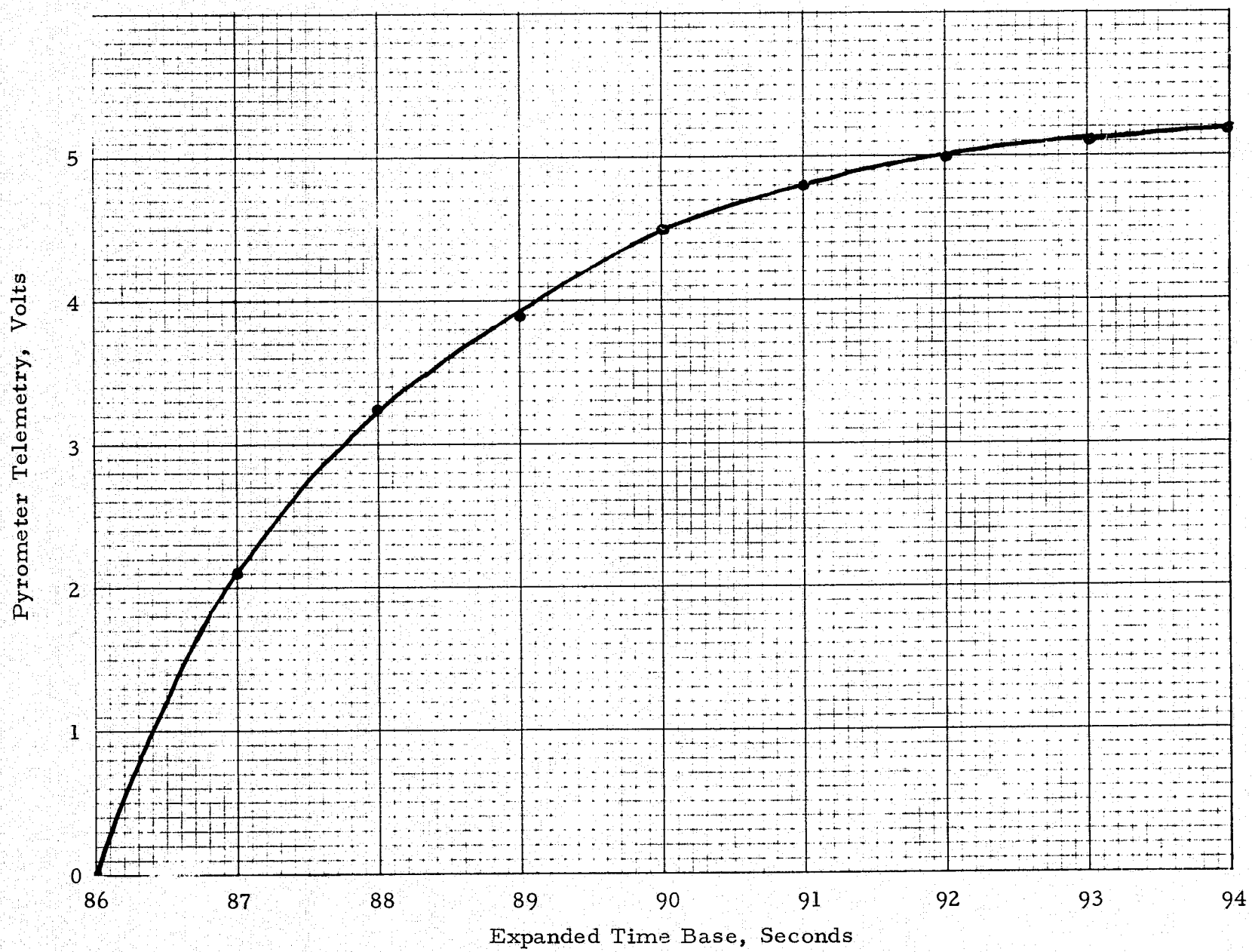

Figure 51. Pyrometer Telemetry Signal, Heating Curve

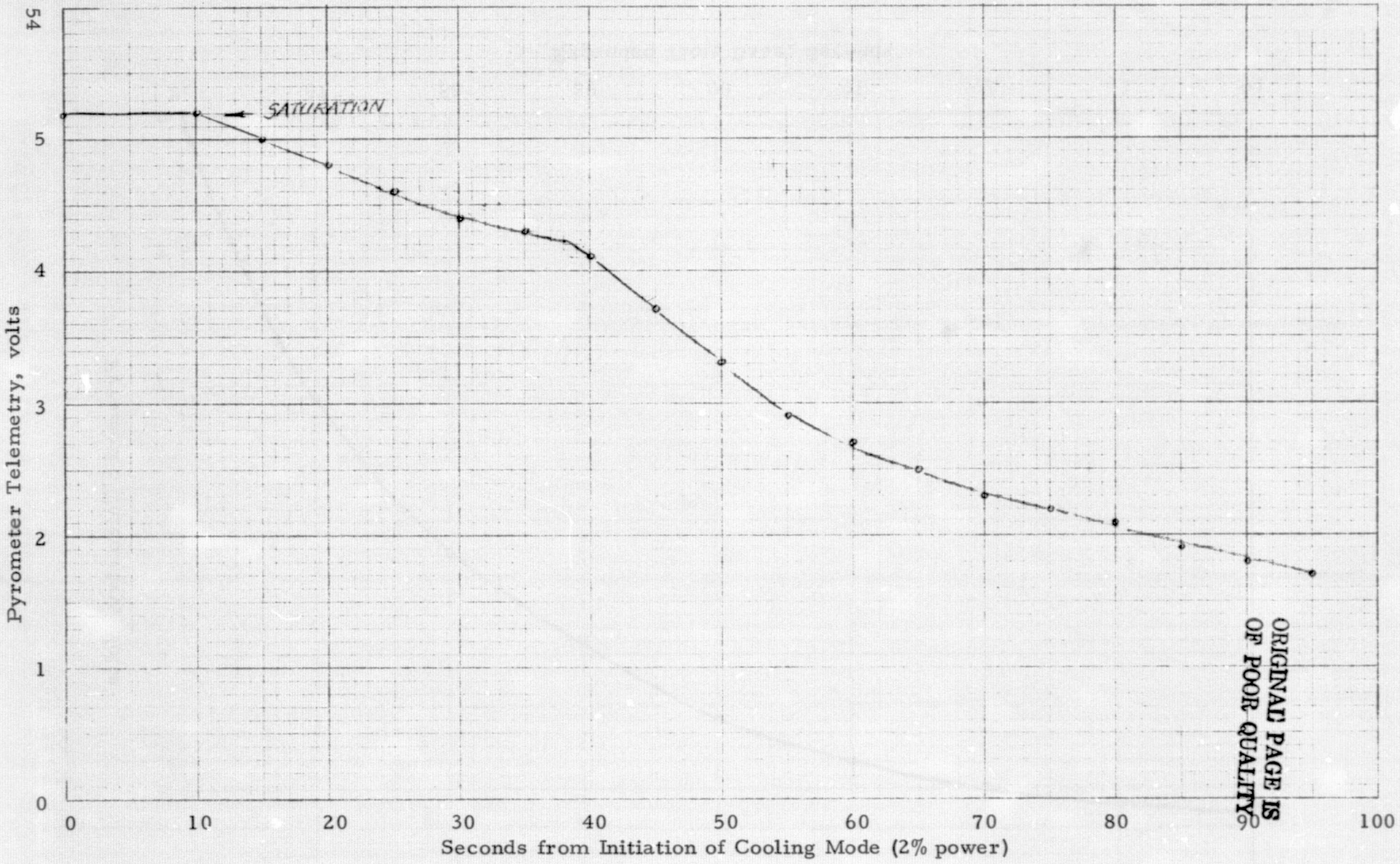

Figure 52. Pyrometer Telemetry Signal, Cooling Curve

Figure 53. Temperature-Time Curve for Flight Specimen

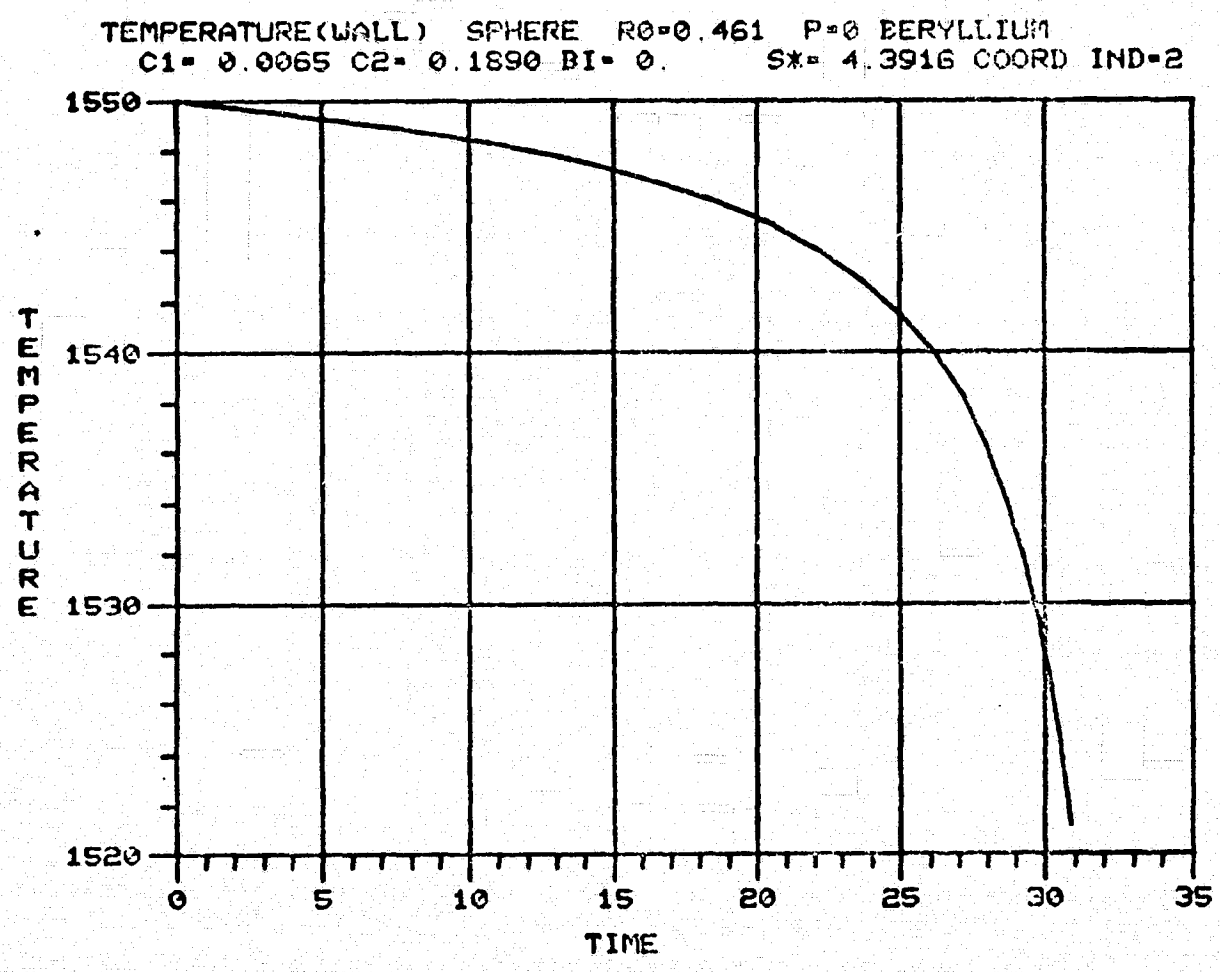
TEMPERATURE(WALL) SPHERE R0=0.461 P=0 BERYLLIUM
C1= 0.0065 C2= 0.1890 BI= 0. S*= 4.3916 COORD IND=2
1550
1540
1530
1520
TEMPERATURE
0
5
10
15
20
25
30
35
TIME

Figure 54

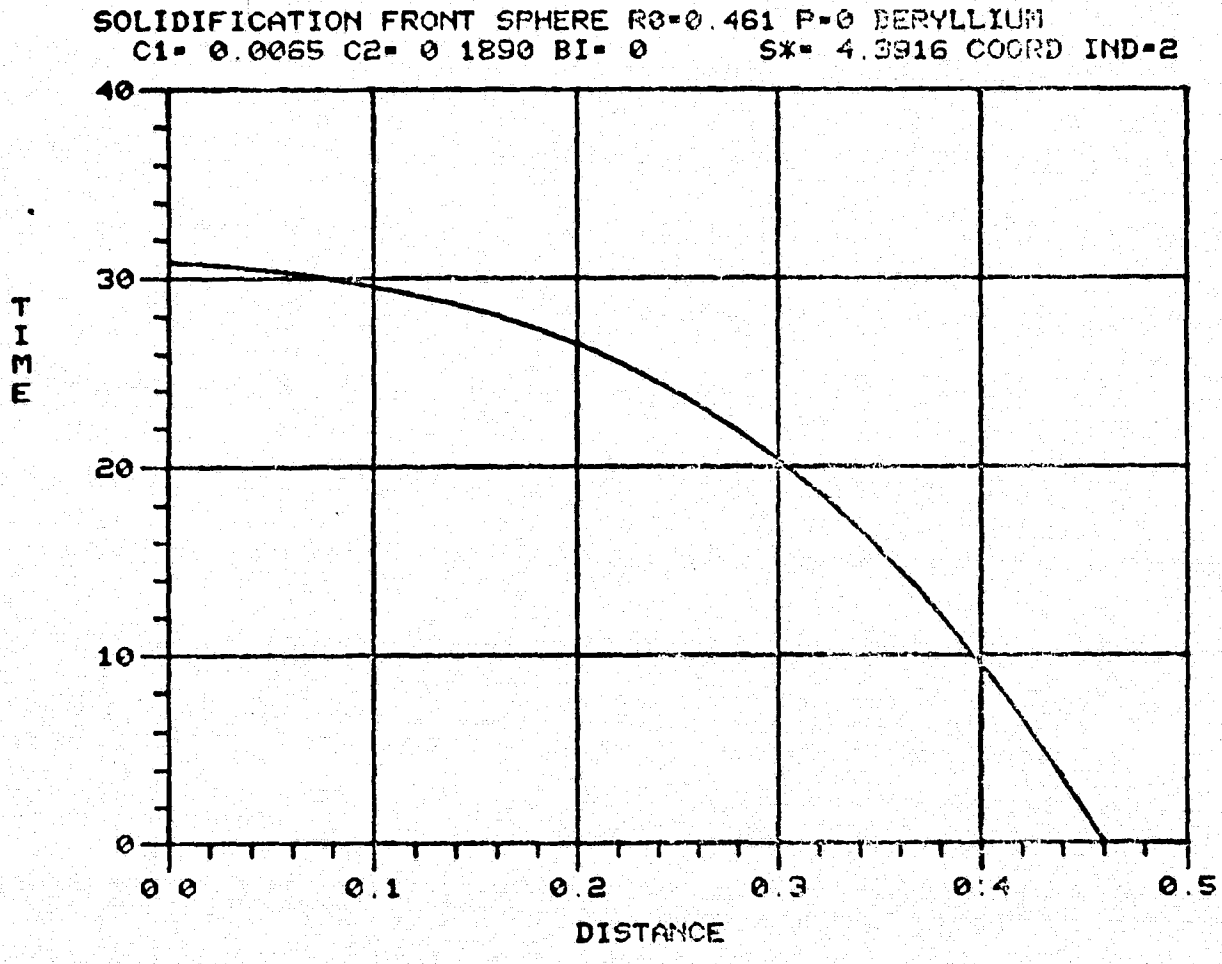
SOLIDIFICATION FRONT SPHERE R0=0.461 P=0 BERYLLIUM
C1= 0.0065 C2= 0 1890 BI= 0 S*= 4.3916 COORD IND=2
40
30
20
10
0
TIME
0 0
0.1
0.2
0.3
0.4
0.5
DISTANCE

Figure 55

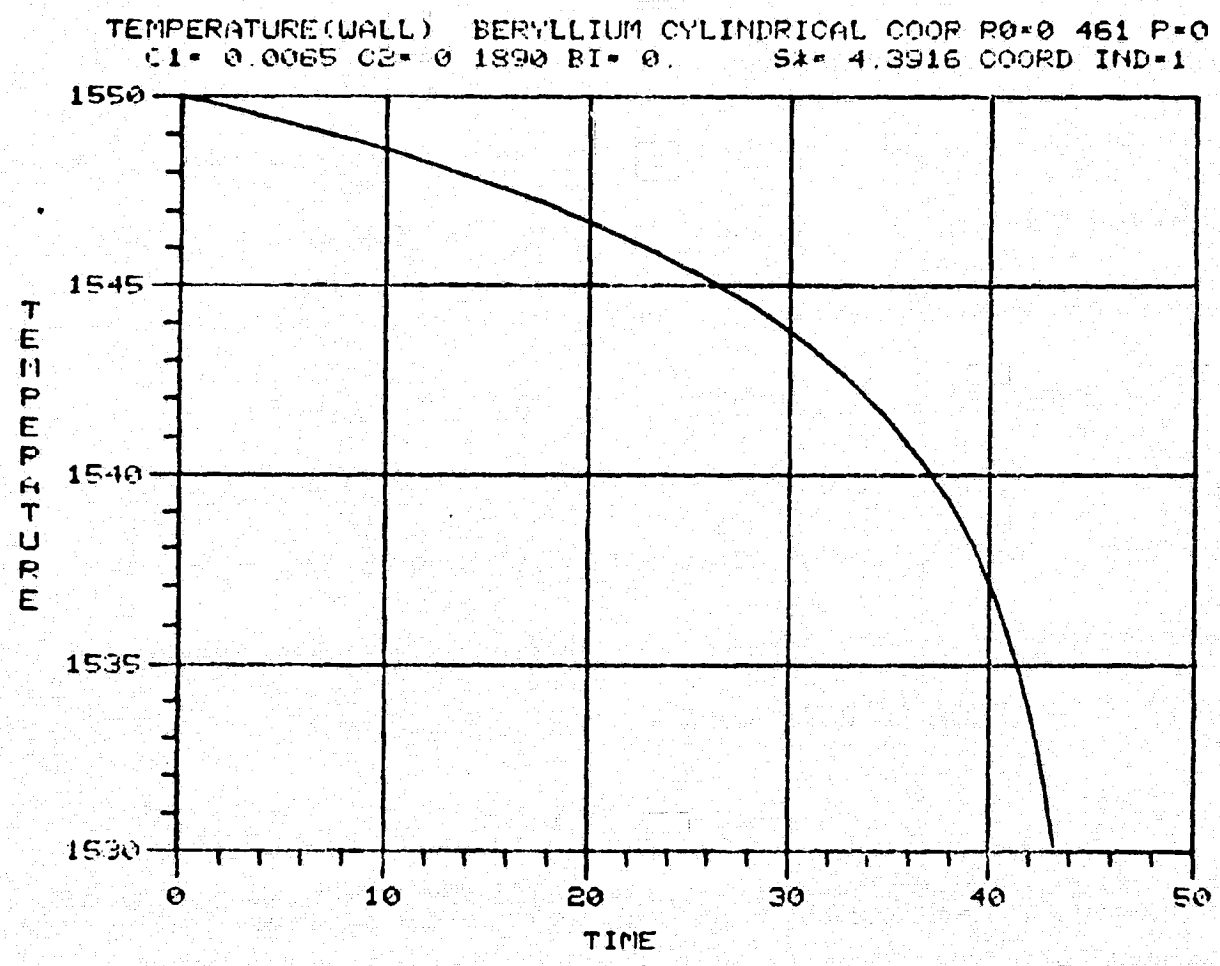
TEMPERATURE(WALL) BERYLLIUM CYLINDRICAL COOR R0=0 461 P=0
C1= 0.0065 C2= 0 1890 BI= 0. S*= 4.3916 COORD IND=1
1550
1545
1540
1535
1530
TEMPERATURE
0
10
20
30
40
50
TIME

Figure 56

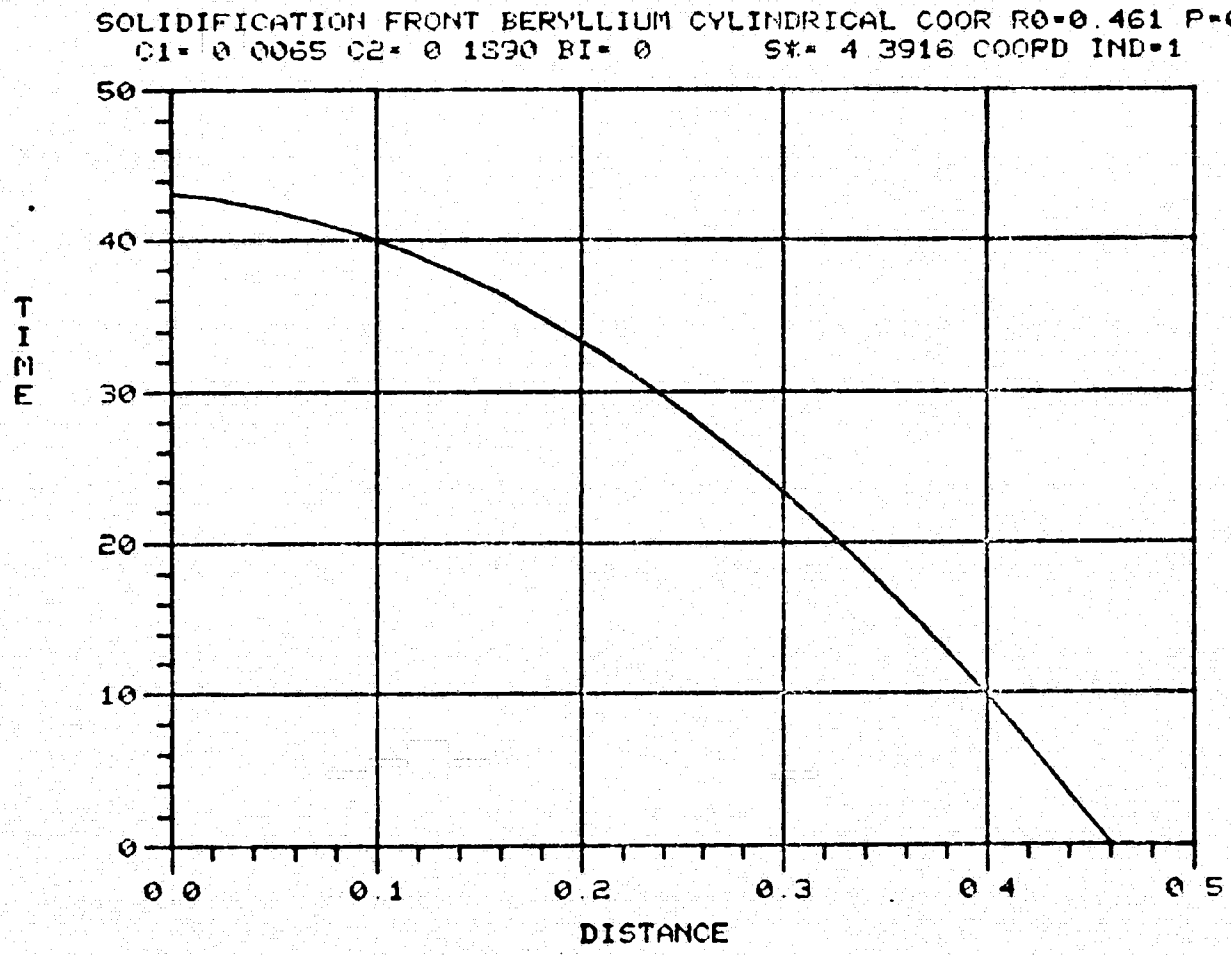
SOLIDIFICATION FRONT BERYLLIUM CYLINDRICAL COOR R0=0.461 P=0
C1= 0 0065 C2= 0 1390 BI= 0 S*= 4 3916 COORD IND=1
TIME
50
40
30
20
10
0
0 0
0.1
0.2
0.3
0 4
0 5
DISTANCE

Figure 57

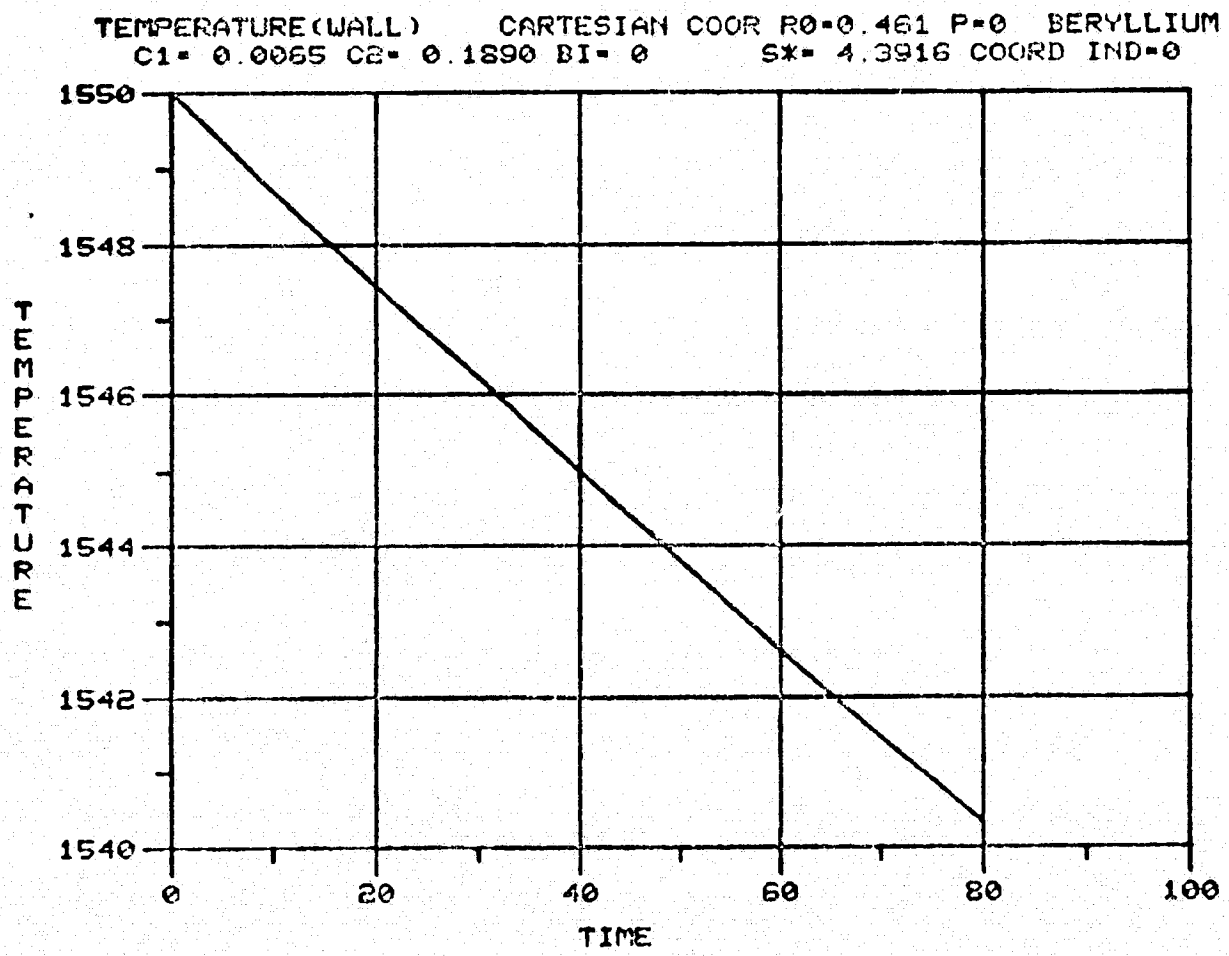
TEMPERATURE(WALL) CARTESIAN COOR R0=0.461 P=0 BERYLLIUM
C1= 0.0065 C2= 0.1890 BI= 0 S*= 4.3916 COORD IND=0
1550
1548
1546
1544
1542
1540
TEMPERATURE
0
20
40
60
80
100
TIME

Figure 58

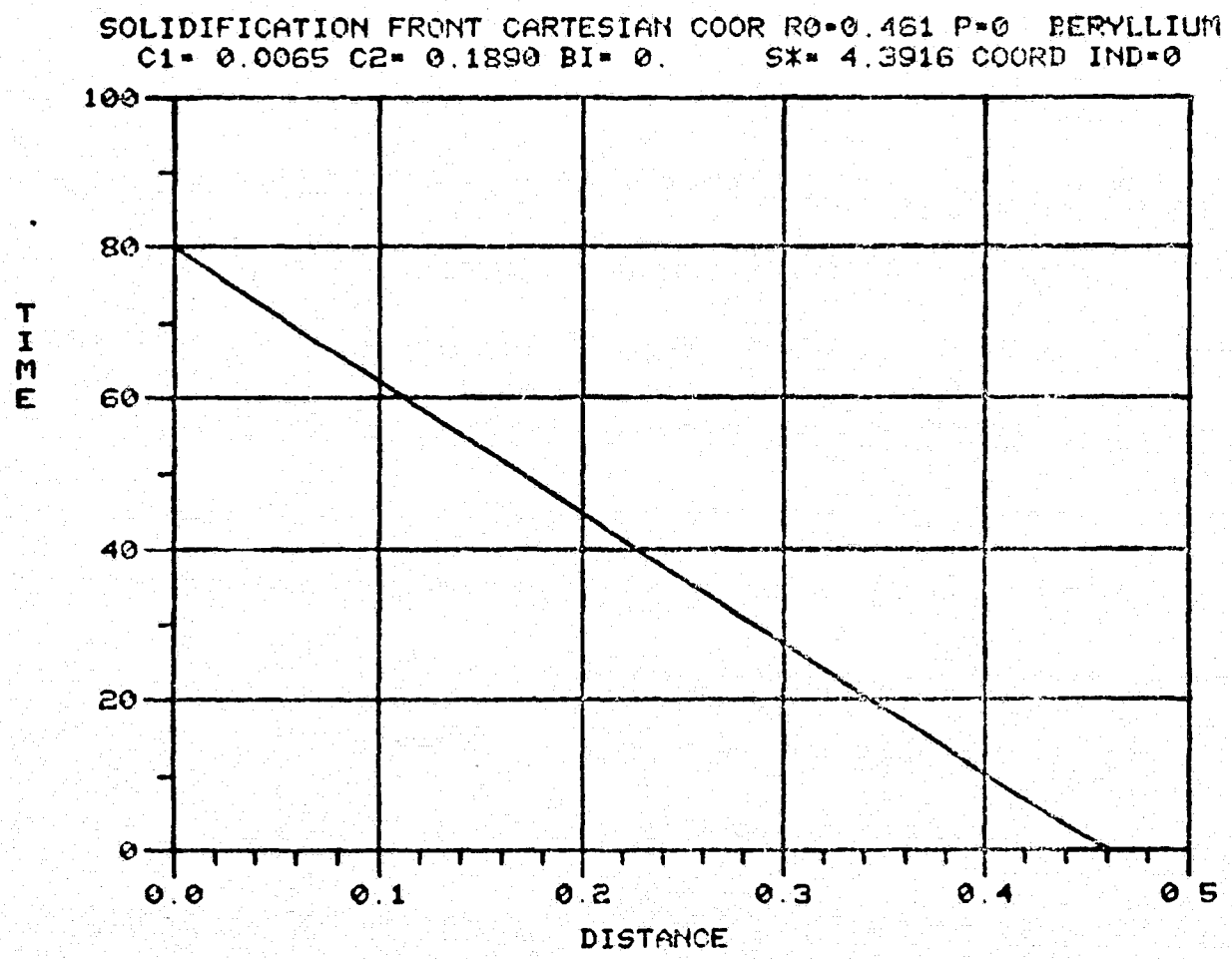
SOLIDIFICATION FRONT CARTESIAN COOR R0=0.461 P=0 BERYLLIUM
C1= 0.0065 C2= 0.1890 BI= 0. S*= 4.3916 COORD IND=0
100
80
60
40
20
0
TIME
0.0
0.1
0.2
0.3
0.4
0.5
DISTANCE

Figure 59

APPENDIX B

AGGLOMERATION AND SEPARATION OF BERYLLIA FROM BERYLLIUM MELTS

Agglomeration and separation are hypothesized to occur primarily due to collisions between beryllia particles in the melt. These collisions occur due to (1) the settling of BeO particles due to their density difference in the melt and (2) fluid motion sweeping BeO particles together. The first is called Stokes collisions. The larger BeO particles, settling fastest, collect smaller particles. The second is called Velocity Gradient Collisions and collisions occur between particles of equal size as well as particles of unequal size.

Lindborg and Torsell[3] developed a statistical model for these types of collisions. Using their results, agglomeration and separation times of 1 minute or less are likely for BeO particles ranging in size from 0.2 to 1.3 μm in specimens of beryllium melted in the terrestrial environment. In the weightless environment of space, where the accelerations due to gravity are reduced by a factor of 10^4, the frequency of Stokes Collisions is reduced proportionately, as the velocity of settling is directly proportional to the acceleration due to gravity. While all fluid motions, i.e. stirring, are not reduced in the weightless environment of space, fluid motion due to gravity driven convection is reduced. Thus agglomeration and separation times might be extended to periods of many hours or days in the weightless environment of space. It is hypothesized that the much more uniform dispersion obtained in the flight specimen due to the reduction in collision frequency for BeO particles in the weightless environment of space.